

THE STUDY OF IN VITRO SUPERFUSED SPIRAL MODIOLAR ARTERY BIOASSAY ON  
THE ENDOTHELIN-1 ANTAGONISTIC ACTIVITY OF (+)-MYRICERIC ACID A AND ITS  
NOVEL SYNTHETIC TETRACYCLIC TERPENOIDS INTERMEDIATES

by

WEIER BAO

Bachelor of Medicine, Dalian Medical University, 2007

A THESIS

submitted in partial fulfillment of the requirements for the degree

MASTER OF SCIENCE

Department of Chemistry  
College of Arts and Science

KANSAS STATE UNIVERSITY  
Manhattan, Kansas

2010

Approved by:

Major Professor  
Professor Duy H. Hua

# **Copyright**

WEIER BAO

2010

## Abstract

(+)-myriceric acid A is known as a non-peptide ET<sub>A</sub> receptor antagonist. It is isolated from the natural plant *Myrica cerifera* with 0.01% yield which is very low. The total synthesis of (+)-myriceric acid A is being pursued in Hua's lab. (+)-myriceric acid A specifically blocks the vasoconstriction caused by endothelin-1 (ET-1). Because some derivatives of (+)-myriceric acid A were shown to have ET-1 receptor antagonistic effect, the tetracyclic terpenoid intermediates toward the total synthesis of (+)-myriceric acid A are postulated to have the similar antagonistic activities. The objective of this project is to study the release of vasoconstriction of these synthetic intermediates and compare their antagonistic potency.

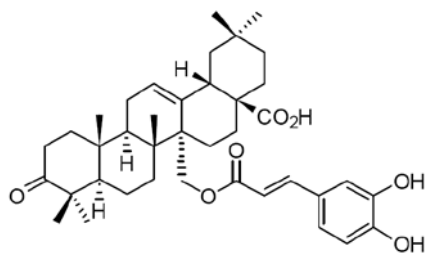
The ET-1 receptor antagonistic bioactivity of six (+)-myriceric acid A intermediates as well as (+)-myriceric acid A were evaluated by the in vitro spiral modiolar artery (SMA) bioassay. The synthetic intermediates which have not been reported in the literature were previously synthesized in Hua's laboratory by Dr. Angelo Aguilar and Dr. Aibin Shi. Their synthesis was described in Dr. Aguilar's PhD thesis. All the antagonistic effect evaluations were based on the SMA's diameter changes. SMA's diameter changes were induced by the superfusion of different extracellular solutions. The dose-response curves and straight lines were plotted to compare the antagonistic potency of these compounds. Based on the EC<sub>50</sub> value of (+)-myriceric acid A intermediates (0.090 μM ~ 0.582 μM for the curves and 0.095 μM ~ 0.385 μM for the straight lines), all of the compounds have ET-1 receptor antagonistic activity, therefore the synthesis and screening of (+)-myriceric acid A intermediates is probably a promising route to develop new non-peptide ET<sub>A</sub> receptor antagonists.

# Table of Contents

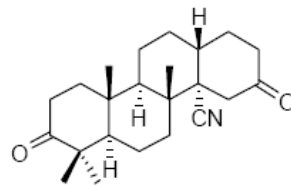
Structures of compounds .....	vi
List of Figures .....	vii
List of Tables .....	ix
List of Graphs .....	x
Acknowledgements.....	xii
Dedication.....	xiii
CHAPTER 1 – Introduction: biological importance of (+)-myriceric acid A and the spiral modiolar artery SMA) bioassay.....	1
1.1 Objective of SMA bioassay.....	1
1.2 Isolation and characterization of (+)-myriceric acid A.....	1
1.3 Chemical modification of (+)-myriceric acid A and structure activity relationships.....	2
1.4 Biological activity of (+)-myriceric acid A .....	3
1.4.1 Endothelins .....	4
1.4.2 Endothelin Receptors .....	7
1.4.3 Proposed mechanism for vasoconstriction caused by ET-1.....	7
1.4.4 Endothelin receptor antagonists .....	10
1.5 Bioassay for determining (+)-myriceric acid A and its intermediates as endothelin receptor antagonists .....	10
1.5.1 Vascular anatomy of SMA and its characteristics .....	11
1.5.2 The diameter of SMA control the blood flow.....	11
CHAPTER 2 – SMA bioassay methods and materials.....	13
2.1 Preparation of solution.....	13
2.2 Isolation and microdissection of SMA .....	14
2.3 Superfusion of SMA .....	14
2.4 Measurement of SMA diameter.....	15
2.5 The results and statistics .....	16
2.6 Pharmacological analysis.....	45
CHAPTER 3 - Discussion .....	55

3.1 Comparison of the drug antagonistic potency based on the current result .....	55
3.2 Some other analysis on the SMA diameter superfusion figures.....	58
3.3 The simultaneous measurement of intracellular Ca <sup>2+</sup> concentration and SMA diameter..	59
CHAPTER 4 – Conclusion and the prospect of the further research .....	62
4.1 Conclusion of the current research .....	62
4.2 improvement of future work .....	62
References.....	63

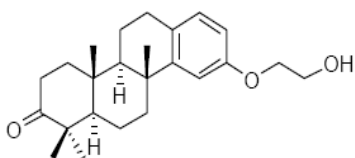
## Structures of Compound



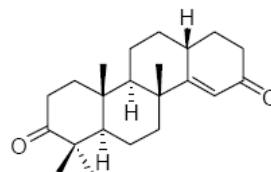
(+)-myriceric Acid A



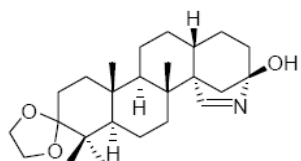
TM-1



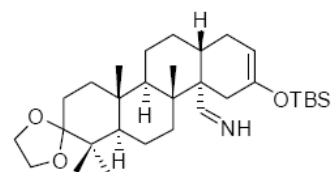
TM-2



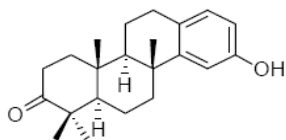
TM-3



TM-4



TM-5



TM-6

## List of Figures

Figure 1	Structure of (+)-myriceric acid A .....	2
Figure 2	(+)-myriceric acid A and its derivatives .....	2
Figure 3	Structures of tetracyclic terpenoid (+)-myriceric acid A intermediates .....	3
Figure 4	Primary structures of endothelins .....	4
Figure 5	Biosynthetic pathway of ET-1 .....	6
Figure 6	Vascular signal transduction mechanism for the smooth muscle cell contraction .....	9
Figure 7	The schematic mechanism for cross bridge circulation .....	10
Figure 8	The schematic diagram of the SMA bioassay experimental work .....	13
Figure 9	SMA diameter changes in superfusion (1.0 $\mu$ M TM-1) .....	16
Figure 10	SMA diameter changes in superfusion (0.3 $\mu$ M TM-1) .....	18
Figure 11	SMA diameter changes in superfusion (0.1 $\mu$ M TM-1) .....	19
Figure 12	SMA diameter changes in superfusion (0.1 $\mu$ M TM-2) .....	21
Figure 13	SMA diameter changes in superfusion (0.3 $\mu$ M TM-2) .....	22
Figure 14	SMA diameter changes in superfusion (1.0 $\mu$ M TM-2) .....	23
Figure 15	SMA diameter changes in superfusion (0.1 $\mu$ M TM-3) .....	24
Figure 16	SMA diameter changes in superfusion (0.3 $\mu$ M TM-3) .....	25
Figure 17	SMA diameter changes in superfusion (0.1 $\mu$ M TM-4) .....	26
Figure 18	SMA diameter changes in superfusion (0.3 $\mu$ M TM-4) .....	27
Figure 19	SMA diameter changes in superfusion (0.5 $\mu$ M TM-4) .....	28
Figure 20	SMA diameter changes in superfusion (1.0 $\mu$ M TM-4) .....	29
Figure 21	SMA diameter changes in superfusion (0.1 $\mu$ M TM-5) .....	30
Figure 22	SMA diameter changes in superfusion (0.5 $\mu$ M TM-5) .....	31
Figure 23	SMA diameter changes in superfusion (1.0 $\mu$ M TM-5) .....	32
Figure 24	SMA diameter changes in superfusion (0.1 $\mu$ M TM-6) .....	33
Figure 25	SMA diameter changes in superfusion (0.3 $\mu$ M TM-6) .....	34
Figure 26	SMA diameter changes in superfusion (1.0 $\mu$ M TM-6) .....	35
Figure 27	SMA diameter changes in superfusion (0.1 $\mu$ M (+)-myriceric acid A) .....	36
Figure 28	SMA diameter changes in superfusion (0.5 $\mu$ M (+)-myriceric acid A) .....	37
Figure 29	SMA diameter changes in superfusion (1.0 $\mu$ M (+)-myriceric acid A) .....	38

Figure 30 Normalized intracellular  $\text{Ca}^{2+}$  concentration and normalized diameter of SMA in the simultaneous measurement experiment ..... 59

Figure 31 The Normalized intracellular  $\text{Ca}^{2+}$  concentration and diameter of SMA in the cumulative simultaneous measurement experiment ..... 60



## List of Tables

Table 1 % of antagonistic activity of TM-1 .....	20
Table 2 % of antagonistic activity of TM-2.....	39
Table 3 % of antagonistic activity of TM-3.....	40
Table 4 % of antagonistic activity of TM-4.....	41
Table 5 % of antagonistic activity of TM-5.....	42
Table 6 % of antagonistic activity of TM-6.....	43
Table 7 % of antagonistic activity of (+)-myriceric acid A .....	44
Table 8 Different compound's EC <sub>50</sub> value.....	54

## List of Graphs

Graph 1: Percentage of 1 nM ET-1 induced constriction in the presence of (+)-myriceric acid A Versus concentration of (+)-myriceric acid A (curve).....	46
Graph 2: Percentage of 1 nM ET-1 induced constriction in the presence of (+)-myriceric acid A Versus concentration of (+)-myriceric acid A (linear) .....	47
Graph 3: Percentage of 1 nM ET-1 induced constriction in the presence of TM-1 Versus concentration of TM-1 (curve).....	48
Graph 4: Percentage of 1 nM ET-1 induced constriction in the presence of TM-1 Versus concentration of TM-1 (linear) .....	48
Graph 5: Percentage of 1 nM ET-1 induced constriction in the presence of TM-2 Versus concentration of TM-2 (curve).....	49
Graph 6: Percentage of 1 nM ET-1 induced constriction in the presence of TM-2 Versus concentration of TM-2 (linear) .....	49
Graph 7: Percentage of 1 nM ET-1 induced constriction in the presence of TM-3 Versus concentration of TM-3 (curve).....	50
Graph 8: Percentage of 1 nM ET-1 induced constriction in the presence of TM-3 Versus concentration of TM-3 (linear) .....	50
Graph 9: Percentage of 1 nM ET-1 induced constriction in the presence of TM-4 Versus concentration of TM-4 (curve).....	51
Graph 10: Percentage of 1 nM ET-1 induced constriction in the presence of TM-4 Versus concentration of TM-4 (linear) .....	51
Graph 11: Percentage of 1 nM ET-1 induced constriction in the presence of TM-5 Versus concentration of TM-5 (curve).....	52
Graph 12: Percentage of 1 nM ET-1 induced constriction in the presence of TM-5 Versus concentration of TM-5 (linear) .....	52
Graph 13: Percentage of 1 nM ET-1 induced constriction in the presence of TM-6 Versus concentration of TM-6 (curve).....	53
Graph 14: Percentage of 1 nM ET-1 induced constriction in the presence of TM-6 Versus concentration of TM-6 (linear) .....	53

Graph 15: Percentage of 1 nM ET-1 induced constriction in the presence of (+)-myriceric acid A  
Versus concentration of (+)-myriceric acid A (limited concentration based on curve)..... 56

Graph 16: Percentage of 1 nM ET-1 induced constriction in the presence of TM-4 Versus  
concentration of TM-4 (limited concentration based on curve) ..... 57

Graph 17: Percentage of 1 nM ET-1 induced constriction in the presence of different compounds  
Versus concentration of different compounds (linear) ..... 58

## Acknowledgements

First I would like to thank my advisor Dr. Hua for giving me the opportunity to study in Kansas State University and his instructions during my graduate study. His enthusiasm on the scientific research inspires me very much. Not only taught me the organic chemistry knowledge, he also purposely guided me thinking actively toward the research. Everyone knowing him is so impressed by his hard working habit and he is definitely an excellent model to learn in my future development.

I also would like to thank my committee members Dr. Klabunde, Dr. Rayat and Dr. Troyer for their suggestions and instructions on my final dissertation. Thanks to Dr. Wangemann for her unselfish collaborative support on my research. I would like to thank the members in Dr. Wangemann's lab: Xiangmin Li, Dr. Kim Dr. Takayuky and Joe.

I would like to thank my previous and current lab mates Dr. Aibin Shi, Dr. Angelo Aguilar, Dr. Sundeep Rana, Allan Prior, Thi Nguyen, Keshar Prasain, Laxman Pokhrel, Mahendra Thapa, Jianyu Lu and Angela Adams for their extensive help.

Finally I would like to thank my parents and my wife for their support in my life. You always encourage me to work toward my goal. Without your love, I would never survive here. I love you so much.

## **Dedication**

I would like to dedicate this thesis to my parents and my wife. Thank you!

# **CHAPTER 1- Introduction: biological importance of (+)-Myriceric acid A and the spiral modiolar artery (SMA) bioassay**

## **1.1 Objective of SMA bioassay**

Several tetracyclic compounds were obtained on route to the total synthesis of (+)-myriceric acid A in Hua's laboratory. These compounds were synthesized by Dr. Angelo Aguilar and Dr. Aibin Shi. The (+)-myriceric acid A intermediates possess a tetracyclic skeleton and several functional groups in (+)-myriceric acid A. Synthesizing a four-ring compound is easier than producing a five-ring compound. Furthermore, some intermediates possess other functional groups which (+)-myriceric acid A does not contain. It would therefore be prudent to test whether these compounds have similar or enhanced biological activity as that of (+)-myriceric acid A. In order to compare the biological activities of these intermediates with (+)-myriceric acid A, its biological function was tested using a spiral modiolar artery (SMA) bioassay. SMA can be induced to constrict by an endothelin-1(ET-1) solution. Other SMAs were superfused by the combinative solution of ET-1 and (+)-myriceric acid A intermediate. If the intermediate compound has ET-1 antagonistic activity, the SMA relative constriction magnitude in the combinative solution will be smaller than that in pure ET-1 solution. By altering the concentrations of the intermediate, a dose-response curve will be obtained and an EC<sub>50</sub> value for the compound can be calculated. Finally, the ET-1 antagonistic potencies can be compared based on their EC<sub>50</sub> values.

## **1.2 Isolation and characterization of (+)-myriceric acid A**

In 1992, Fujimoto and his colleagues at the Shionogi Research Laboratory in Japan reported that (+)-myriceric acid A was isolated from the methanol extract of *Myrica Cerifera* branches and also showed to be a non-peptide endothelin A (ET<sub>A</sub>) receptor antagonist.<sup>1</sup> (+)-myriceric acid A can inhibit an increase of cytosolic free Ca<sup>2+</sup> concentration in Swiss 3T3 fibroblasts and the ET-1 induced contraction of rat aortic strips.<sup>1</sup>

In 1996, researchers in Shionogi Research Laboratory used high resolution liquid secondary ion mass spectrometry (HR-LSI-MS) to deduce the molecular formula of (+)-myriceric acid A that is  $C_{39}H_{52}O_7$ .<sup>2</sup> The structure of (+)-myriceric acid A is shown below (Figure 1) was also deduced by NMR spectroscopy and the X-ray crystallography analysis on its derivatives.<sup>2</sup>

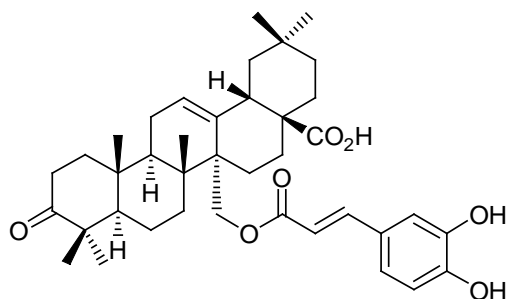


Figure 1. Structure of (+)-myriceric acid A (MA)

### 1.3 Chemical modification of (+)-myriceric acid A and structure activity relationships (SAR)

By modifying the functional groups of (+)-myriceric acid A and comparing the binding affinity of (+)-myriceric acid A derivatives. Fujimoto suggested that four functional groups are important for the endothelin receptor antagonistic activity, namely, the carbonyl group in C-3, the carboxylic acid group in C-17, the trans-caffeoyloxy group at C-27, and the dimethyl groups in C-20.<sup>2</sup> It is noteworthy that the ET-1 antagonistic potency order of the sulfonyl derivatives and (+)-myriceric acid A is 7'-sulfonyl > (+)-myriceric acid A > 6'-sulfonyl > 6',7'-sulfonyl.<sup>2</sup>

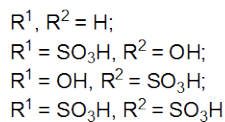
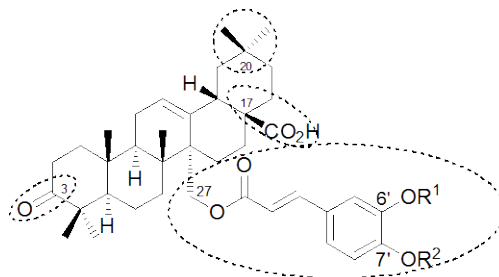


Figure 2. (+)-myriceric acid A and its derivatives<sup>2,3</sup>

Six different tetracyclic terpenoids were synthesized by Dr. Angelo Aguilar. For the convenience of discussion, these tetracyclic terpenoid (+)-myriceric acid A intermediates are named as TM-1, TM-2, TM-3, TM-4, TM-5 and TM-6 respectively, and the structures are showed below (Figure 3). All of these (+)-myriceric acid A intermediates have a four-ring structure. TM-1, TM-2, TM-3 and TM-6 have the carbonyl group on C-3, which may contribute their antagonistic activity. All six intermediates have different functional groups which (+)-myriceric acid A does not possess, however they still possess potential antagonistic effects because their core scaffold which is similar to (+)-myriceric acid A.

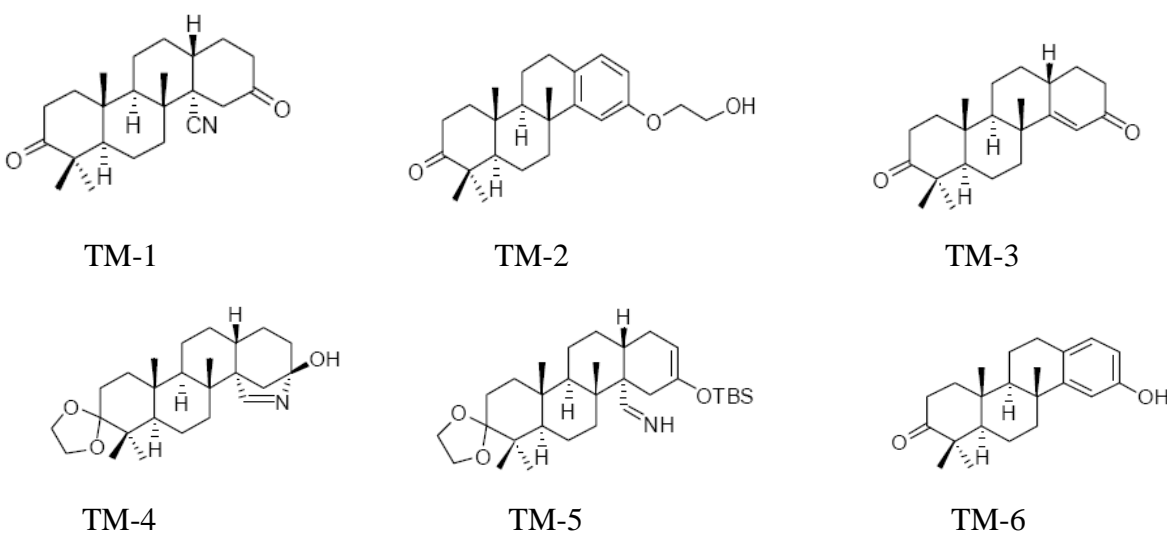


Figure 3. Structures of tetracyclic terpenoid (+)-myriceric acid A intermediates

#### 1.4 Biological activity of (+)-myriceric acid A

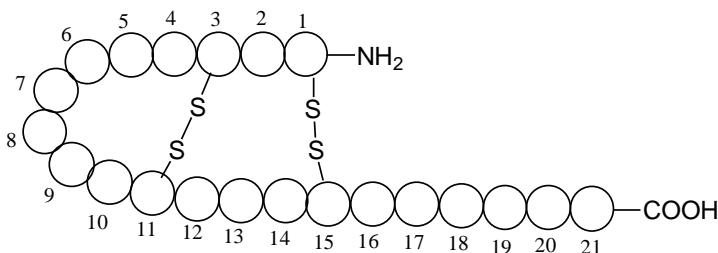
There are three endothelin (ET) isoforms (ET-1, ET-2 and ET-3)<sup>4</sup> and two endothelin receptor isoforms (ET<sub>A</sub> and ET<sub>B</sub> receptors).<sup>5-7</sup> It has been reported that (+)-myriceric acid A can selectively antagonized specific binding of endothelin-1 (ET-1) and not endothelin-3 (ET-3)<sup>2</sup>. Because ET<sub>A</sub> receptor is highly selective for ET-1, and the ET<sub>B</sub> receptor is nonselective for ET-1, ET-2 and ET-3, (+)-myriceric acid A is suggested to act as a non-peptide of ET<sub>A</sub> receptor antagonist.<sup>1</sup> It showed not only the inhibition of ET-1-induced increased in cytosolic Ca<sup>2+</sup>



concentration ( $IC_{50} = 11 \pm 2$  nM) but also ET-1 binding to cells in rat aortic smooth muscle A7r5 Cells ( $K_i = 66 \pm 15$  nM).<sup>2</sup> Next is the brief introduction about endothelins, endothelin receptors, endothelin receptor antagonists and their relationships.

### 1.4.1 Endothelins

In 1988, Yanagisawa *et al.* first reported that endothelin-1 which is a 21-amino acid polypeptide can be purified from porcine aortic endothelial cells.<sup>8</sup> This polypeptide is also one of the most potent vasoconstrictors known.<sup>3</sup> In 1989 Inoue *et al.* found that endothelins have three isoforms: ET-1, ET-2 and ET-3.<sup>4</sup> All of the these isoforms are 21 amino-acid polypeptides containing two disulfide linkages (Cys1-Cys15 and Cys3-Cys11) and they are encoded by three separated genes.<sup>9</sup> Compared with ET-1, ET-2 and ET-3 have 2 and 6 different amino acids respectively. The structures are showed in Figure 4<sup>9</sup>.



Endothelin-1: Cys-Ser-Cys-Ser-Ser-Leu-Met-Asp-Lys-Glu-Cys-Val-Tyr-Phe-Cys-His-Leu-Asp-Ile-Ile-Trp

Endothelin-2: Cys-Ser-Cys-Ser-Ser-Trp-Leu-Asp-Lys-Glu-Cys-Val-Tyr-Phe-Cys-His-Leu-Asp-Ile-Ile-Trp

Endothelin-3: Cys-Thr-Cys-Phe-Thr-Tyr-Lys-Asp-Lys-Glu-Cys-Val-Tyr-Tyr-Cys-His-Leu-Asp-Ile-Ile-Trp

Figure 4. Primary structures of endothelins<sup>9</sup>

ET-1 is expressed in numerous vascular and nonvascular cells.<sup>10</sup> ET-2 is plentiful in the gastrointestinal tract, and ET-3 exist fairly amount in neuronal tissues.<sup>11,12</sup> ET-1 is the only isoform to be detected in vascular endothelial cells and therefore explains why ET-1 is the primary circulating isoform. It therefore attracts the most attention as compared with the other

isoforms.<sup>11,12</sup> The ET-1 induced contraction of porcine coronary artery strips is long-lasting and characteristically difficult to be removed by washing with physiological solution.<sup>8</sup> ET-1 is more potent and produces longer-acting contractions than angiotensin II and thrombin.<sup>13</sup> Infusion of ET-1 to animals can result a strong vasoconstrictory response and it will maintain 2 hours after infusion of ET-1.<sup>9</sup> ET's chemical structure characteristics are summarized below: firstly, ET's amino acid sequence determines the conformations. Moreover, the molecules contain two pairs of disulfide linkages which make the molecule bend and form a bicycle structure in the center. If the disulfide bonds are broken, ET's bioactivities will decrease significantly. Therefore, the disulfide structure is quite important for maintaining ET's bioactivities.<sup>14-16</sup> Finally, the tail of the peptide which consisted of hydrophobic amino acids also contributes the bioactivities. If the last 5 amino acids are eliminated, the compound completely lose its bioactivities.<sup>14-16</sup>

Figure 5<sup>9</sup> is the main biosynthesizing scheme. Under stress conditions such as hypoxia and myocardial ischemia, endothelin genes in human and animals can be activated by hormone, TGF- $\beta$ , vasopressin, etc. then express preproET. PreproET can be cleaved by specific endopeptidase to form big endothelin.<sup>9,17</sup> Finally, big endothelin is transferred by endothelin converting enzyme (ECE).<sup>9,17</sup> In general, release of endothelin can be mediated by many elements. Under normal physiological conditions, the amount of ET's biosynthesis and release is quite low. Physical and chemical agents in internal milieu, endogenous and exogenous bioactive compounds can influence ET's expressing and releasing.<sup>9,17</sup>

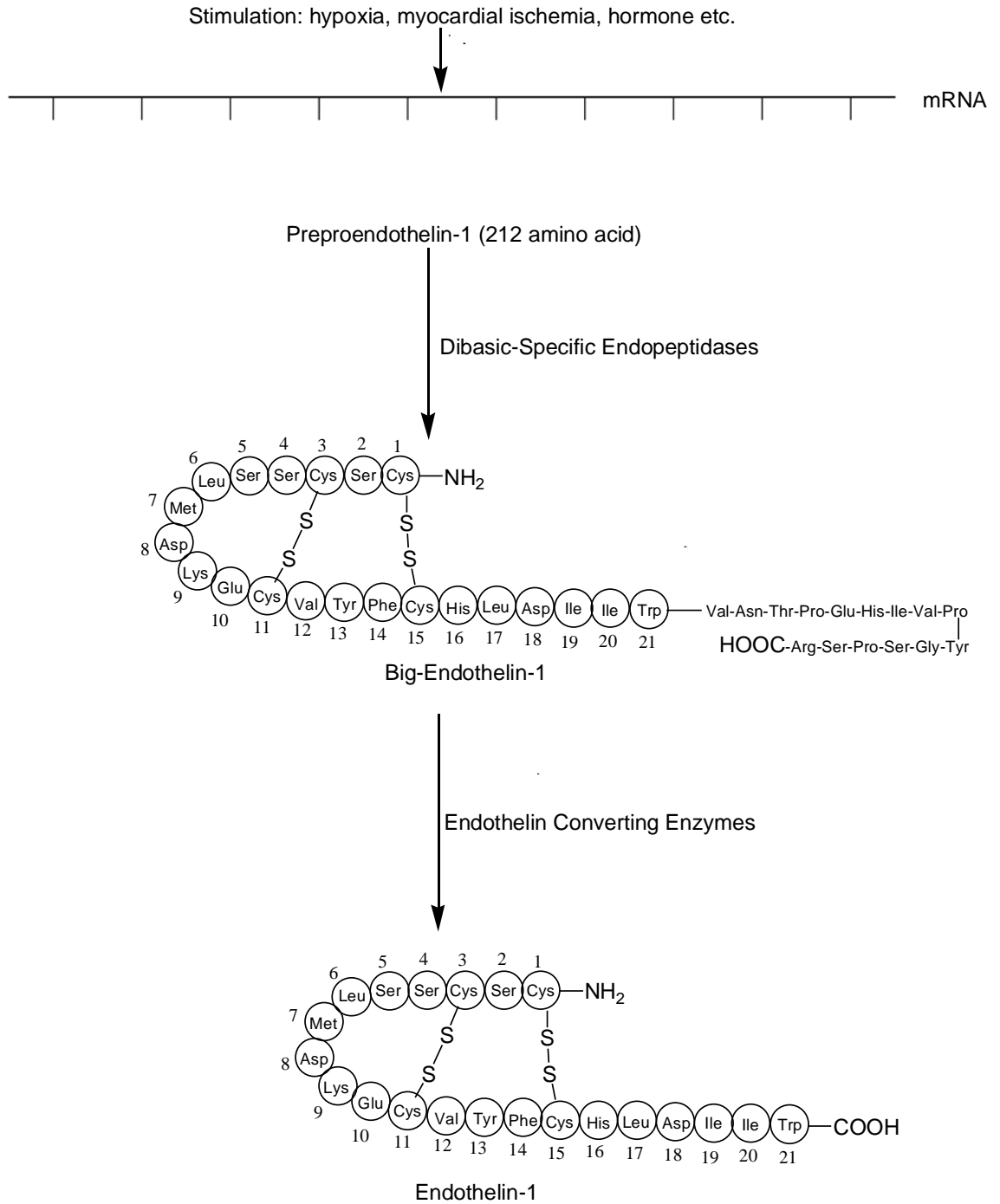


Figure 5. Biosynthetic pathway of ET-1<sup>9</sup>

### ***1.4.2 Endothelin Receptors***

There are two endothelin receptor subtypes that mediate vasoconstriction:  $ET_A$  and  $ET_B$  receptors.<sup>5-7</sup> The endothelin receptors belong to the family of G-protein coupled receptors.<sup>9</sup>  $ET_A$  receptors are found in many tissues, but are particularly abundant in vascular smooth muscle cells in which they exert a vasoconstrictory activity ( see mechanism in Chapter 1.4.3) upon binding of ET-1.<sup>9</sup>  $ET_B$  receptors are widely distributed in endothelial cells and can cause vasodilation.<sup>2,8</sup>  $ET_B$  receptors also exist in vascular smooth muscle cells where they can regulate the vasoconstriction activities.<sup>18-20</sup> Both  $ET_A$  and  $ET_B$  receptors can mediate the vasoconstriction and vasodilation. Meanwhile, the rank order of potency for vasoconstriction was  $ET-1 \geq ET-2 \gg ET-3$  and for vasodilation was  $ET-1 = ET-2 = ET-3$ .<sup>21</sup> These facts indicate that the vasoconstriction and vasodilation of different endothelins are mediated by different endothelin receptor systems.<sup>9</sup> The proposed mechanism for vasoconstriction is demonstrated below.  $ET_B$  receptors can induce the release of NO molecule and prostacyclin which are effective vasodilators.<sup>22</sup> The main pharmacological distinction between  $ET_A$  and  $ET_B$  receptors is that  $ET_A$  receptor is highly selective for ET-1 and the  $ET_B$  receptor is nonselective for ET-1, ET-2 and ET-3. Therefore, ET-1 and its major receptor  $ET_A$  attract most attention than other endothelins and  $ET_B$ .

### ***1.4.3 Proposed mechanism for vasoconstriction caused by ET-1***

Smooth muscle contraction is regulated by the cytosolic free  $Ca^{2+}$  concentration.<sup>23</sup> For example,  $ET_A$  receptors are widely distributed in vascular smooth muscle cells. When ET-1 solution is superfused to the SMA section,  $ET_A$  receptors can specifically identify ET-1 and bind together. The nerve impulse is generated and transmitted to axon tip, the contacting membrane is depolarized to make calcium channel open.<sup>24</sup> Small amount of extracellular  $Ca^{2+}$  which is called activator  $Ca^{2+}$  enter the cells. Because the influx of extracellular  $Ca^{2+}$  activates the voltage-dependent  $Ca^{2+}$  channels which are proteins essentially, the activated  $Ca^{2+}$  channels lead to the consecutive electrical signal transductions, so the influx  $Ca^{2+}$  is called activator calcium.<sup>27,28</sup> The subsequent response of the cell is to increase phospholipase C activity via coupling through a G-

protein.<sup>23,25</sup> Phospholipase C produces two potent messengers from the membrane lipid phosphatidylinositol 4,5-bisphosphate: inositol 1,4,5-trisphosphate (IP3) and diacylglycerol (DG).<sup>23,26</sup> IP3 binds to specific receptors on the sarcoplasmic reticulum and stimulates the release of activator calcium ( $\text{Ca}^{2+}$ ). DG can activate protein kinase C (PKC) which phosphorylates specific target proteins.<sup>23,26</sup> In most smooth muscles, PKC has contraction-promoting effects such as phosphorylation of  $\text{Ca}^{2+}$  channels or other proteins that regulate cross-bridge cycling (Figure 7, mechanism see below).<sup>23</sup> Activator  $\text{Ca}^{2+}$  binds to calmodulin, leading to activation of myosin light chain kinase (MLC kinase).<sup>23,29</sup> This kinase phosphorylates the myosin light chain (MLC) then MLC combines with actin.<sup>23</sup> The cross-bridge cycling occurs to shorten the smooth muscle cell.<sup>23</sup> It is important to understand the role of cross-bridge cycling in the mechanism of smooth muscle contraction. Figure 7<sup>30</sup> demonstrated the circulation process. In the first step in the graph, the actin-myosin bridge dissociates very quickly because of the binding between ATP to myosin.<sup>30</sup> Then the free myosin bridge and its hydrolysis products recombine with the actin filament.<sup>30</sup> When ATP is being hydrolyzed, the free myosin bridge finds the right position to attach to actin.<sup>30</sup> Finally, the cross-bridge generates force, and actin displaces the reaction products (ADP and Pi) from the myosin cross-bridge. This is the rate-limiting step of contraction.<sup>30</sup> The actin-myosin cross-bridge is now ready for the ATP binding of step 1. It is a circulation.

In 2005, Yoshihiko *et al.* reported that endothelin-1 induced translocation of RhoA was mediated by endothelin  $\text{ET}_A$  receptors in rat bronchial smooth muscle,<sup>31</sup> so a  $\text{Ca}^{2+}$  sensitizing mechanism was proposed: it is initiated at the same time that phospholipase C is activated, and it involves the activation of the small GTP-binding protein RhoA.<sup>23</sup> How to activate RhoA by the G-protein-coupled receptor is not clear presently, but guanine nucleotide exchange factor (RhoGEF) is related in the process.<sup>23</sup> After activation of RhoA, the amount of Rho kinase activity increases.<sup>23</sup> The increased Rho kinase will phosphorylate and deplete the active myosin phosphatase to inactive myosin phosphatase.<sup>23</sup> Because the high-energy phosphate on the contracted MLC-actin complex can be removed by active myosin phosphatase to form a relaxed MLC state, the increased inactive myosin phosphatase can promote the contractile state.<sup>23</sup>

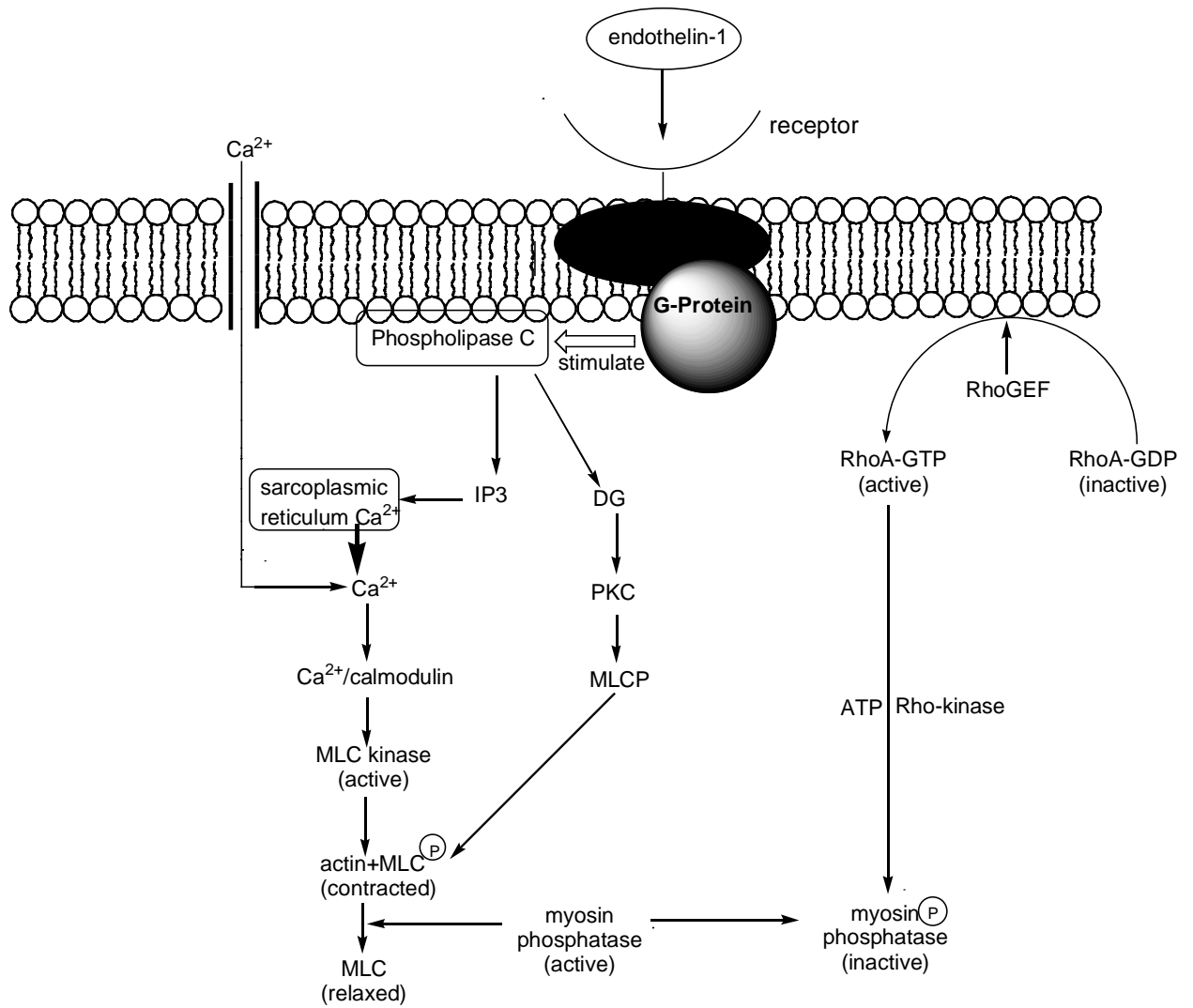


Figure 6. Vascular signal transduction mechanism for the smooth muscle cell contraction<sup>23</sup>

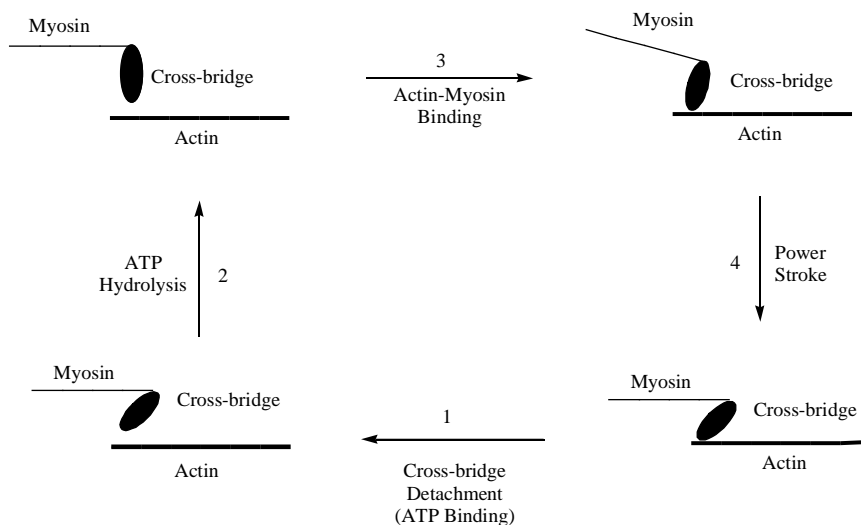


Figure 7. The schematic mechanism for cross bridge circulation<sup>29</sup>

#### 1.4.4 Endothelin receptor antagonists

Based on the structure properties, endothelin receptor antagonists can be categorized two types, peptide based and non peptide based.<sup>9</sup> Due to the existence of two types of endothelin receptors (ETA and ETB receptors), the endothelins can also be divided into selective and non-selective antagonist. Nonselective antagonists which target these two receptor subtypes would presumably exert a greater anti-hypertensive effect than ETA receptor-selective antagonists alone.<sup>9</sup> In contrast, the primary mediator of vasoconstriction is the ETA receptor,<sup>32</sup> so ETA receptors selective antagonist may be preferable to a nonselective agent to manage hypertension.<sup>9</sup> Although several peptide endothelin receptors like BQ123 antagonist have been reported,<sup>33</sup> they have obvious limitation on the pharmacological metabolism stability *in vivo*. Discovering or developing selective non-peptide endothelin receptor antagonists is probably much more favorable for drug discovery.

### 1.5 Bioassay for determining (+)-myriceric acid A and its intermediates as endothelin receptor antagonists

Wangemann *et al.* developed a bioassay to verify that superfusion of ET-1 on spiral modiolar artery (SMA) can induce a transient cytosolic  $\text{Ca}^{2+}$  concentration increases via  $\text{ET}_A$  receptor and a long-lasting vasoconstriction of SMA without ET-1.<sup>34</sup> This project uses this bioassay to test (+)-myriceric acid A and the synthetic intermediates' antagonistic potencies. (+)-myriceric acid A's synthetic intermediates are postulated as potential antagonists. Thus this special bioassay is applied to test their potencies.

### ***1.5.1 Vascular anatomy of SMA and its characteristics***

The spiral modiolar artery derives from the anterior inferior cerebellar artery from the basilar artery and provides the main blood supply to the cochlea.<sup>34</sup> The scala in cochlea is also spiral fashion. The heliciforms from bottom to top are divided three parts, scala tympani, scala media and scala vestibule. The spiral modiolar artery hides at the bottom of the scala tympani. Endothelins have been demonstrated to be present in the cochlea and can cause a reduction cochlear blood flow.<sup>36,37</sup> This reduction cochlear blood flow may be partially due to an  $\text{ET}_A$  receptor mediated vasoconstriction of capillaries in the spiral ligament of the lateral cochlear wall.<sup>38</sup> Ghandour *et al.* inferred the existence of  $\text{ET}_B$  receptors in SMA because  $\text{ET}_B$  receptor antagonists BQ-788 can inhibit the vasoconstriction caused by ET-3.<sup>39</sup> However, it is reported that the elevation of  $\text{ET}_B$  receptor agonist sarafotoxin S6c had no significant vasoconstriction effect on SMA.<sup>34</sup> Therefore, the facts above indicate the amount of  $\text{ET}_B$  receptor in SMA is very tiny. Because the blood flow depends mainly on the vascular diameter which is set by the contractile status of the vascular smooth muscle cells,<sup>36</sup> and the wall of spiral modiolar artery contains single layer of vascular smooth muscle cells and a single layer of endothelin cells.<sup>18</sup> The spiral modiolar artery is an ideal model to access to the  $\text{ET}_A$  receptor.

### ***1.5.2 The diameter of SMA controls the blood flow***

Vasospasm of the spiral modiolar artery probably is the major factor that can cause sudden hearing loss which is the major symptom for the inner ear ischemic stroke.<sup>35</sup> Furthermore, the SMA provides the main blood supply to the cochlea and vascular diameter is the most effective means of controlling blood flow.<sup>35,38,42</sup> Thus it is important to understand basic theory that how the vascular diameter changing can influence the blood flow. Mechanisms



involved in the control of cochlear blood flow include modulation of the perfusion pressure.<sup>38,40,42</sup>

$$F = \Delta P/R \quad (\text{Ohm's Law}) \quad (\text{equation 1})$$

$$R = 8\eta l/\pi r^4 \quad (\text{Hagen-Poiseuille's Law}) \quad (\text{equation 2})$$

F represents blood flow,  $\Delta P$  is the perfusion pressure, R is resistance,  $\eta$  is viscosity, l is the length of blood vessel and r is the radius of vessel.

After combining above two equations, Equation  $F = \Delta P \pi r^4 / 8\eta l$  is obtained. If the diameter decreases, the blood flow will also decrease and vice versa. Therefore, it is important to study the relationship between the diameter of blood vessel and the constrictions.

## Chapter 2 Methods and Materials

All the experimental procedures followed Figure 10 demonstrated below:

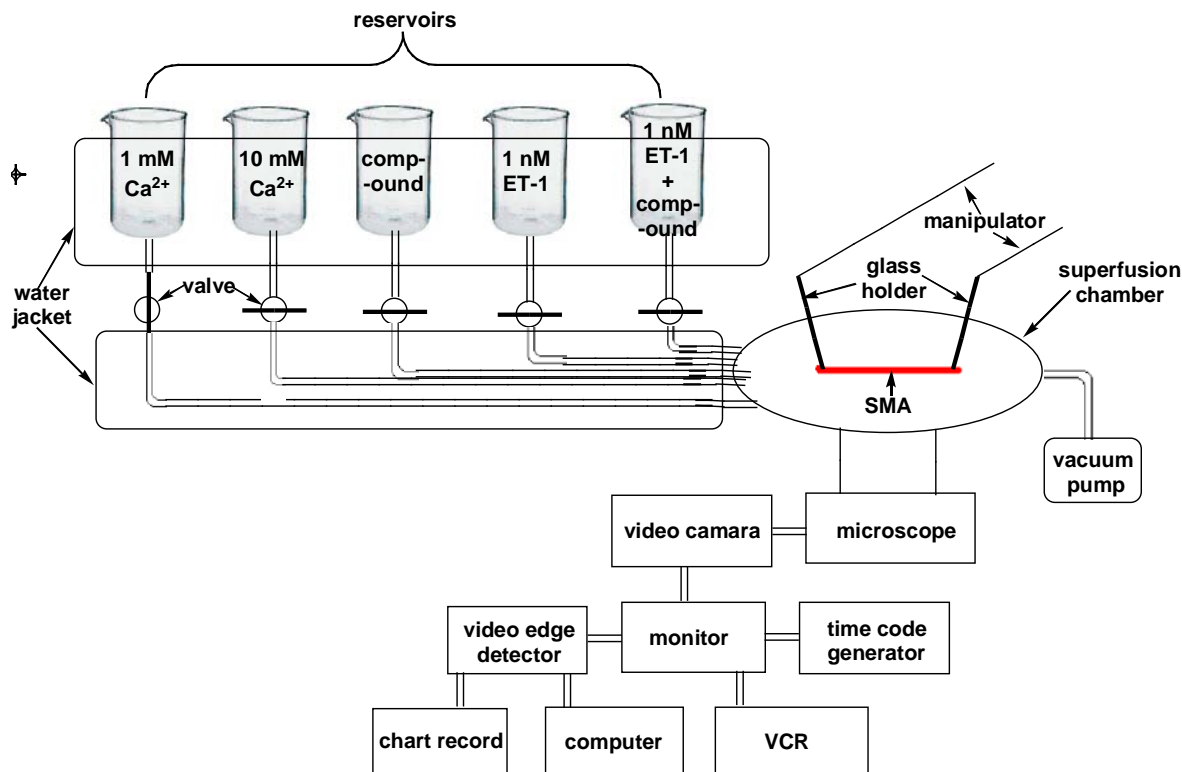


Figure 8. the schematic diagram of the SMA bioassay experimental work<sup>3</sup>

### 2.1 Preparation of solution

To test the compounds (including myriceric acid A and its intermediates), five physiological solutions need to be prepared:

1. A 2 liter of 1.0 mM Ca<sup>2+</sup> physiological salt solution contained 17.532 g of NaCl, 2.383 g of HEPE, 7.2 ml of 1 M KCl, 10 ml of 200 mM MgCl<sub>2</sub>, 14.28 ml of 140 mM CaCl<sub>2</sub> and 1.802 g of glucose (The abbreviation name of this solution is 1 mM Ca<sup>2+</sup> solution in this paper).
2. A 2 liter of 10 mM Ca<sup>2+</sup> physiological salt solution contained 17.532g of NaCl, 2.383 g of HEPE, 7.2 ml of 1 M KCl, 10 ml of 200 mM MgCl<sub>2</sub>, 142.8 ml of 140 mM CaCl<sub>2</sub> and 1.802 g of glucose (The abbreviation name of this solution is 10 mM Ca<sup>2+</sup> solution in this paper).
3. An X μM (X value can be variable according to the concentration of drug we need to test) drug solution, in which the drug is dissolved in the 1 mM Ca<sup>2+</sup> solution

4. A 1 nM ET-1 solution is prepared as below: 10  $\mu\text{g}$  of ET-1 is firstly dissolved in 2 ml  $\text{H}_2\text{O}$ , then 200  $\mu\text{l}$  of this ET-1 water solution is taken out and dissolved again in 400 ml of 1 mM Ca solution.

5. The combination solution of X  $\mu\text{M}$  drug and 1 nM ET-1, in which the drug and ET-1 are dissolved in the 1 mM  $\text{Ca}^{2+}$  solution.

All solutions' PH degree should be adjusted to 7.4

## **2.2 Isolation and microdissection of SMA**

All the SMAs were isolated from Mongolia Gerbils under the protocol approved by the institutional Animal Care and Use Committee at Kansas State University (Protocol Number: 2613). The gerbils were firstly administrated 4% tribromoethanol (TBE) to anesthetize (10  $\mu\text{l}/\text{g}$ ). The weight of a gerbil is approximately 40 - 60 g. The gerbil lost the reaction on the pinching stimulation after the TBE administration, and then it was decapitated. Two temporal bones were taken out from the back of the ear and carefully removed the excess tissues. Then the cochlea was separated from the temporal bones and quickly transferred into a microdissection chamber which was already filled about 5 ml of 1 mM  $\text{Ca}^{2+}$  solution at 4°C. All the dissection work was done under the microscope. The abundant bones surrounding the cochlea were firstly removed. Then the top of the cochlea will be cracked by the dissection scissor and gradually removed the cochlea shell fragments. The SMA was seen through the tiny bone surrounding the modiolaris. After removing the bone around the modiolaris, the SMA which was loosely attached to the nerves was separated. Care was taken so as to not stretch the SMA too much, or it will lose its physiological elasticity. Finally, SMA were cut into small segments. The length of each segment was 200 – 600  $\mu\text{m}$ .

## **2.3 Superfusion of SMA**

Each segment of SMA was transferred into a bath chamber mounted on the stage of an inverted microscope. The chamber was filled with 1 ml of 37°C 1 mM  $\text{Ca}^{2+}$  solution. Then the SMA was held by two blunted glass tips mounted with a micromanipulator that can maneuver

the fixation position on SMA. The chamber connected with 5 containers which filled with different solutions (5 solutions introduced in this paper Chapter 2.1) respectively. By altering the position of the switcher as Figure 8 showed, the solutions in containers will automatically flow through the pipes connected with containers and fill into the chamber. Another vacuum pipe on the other side of the chamber will suck away the solution flowed in. Eventually the mounted vessel segment was superfused at the power balance between solution gravity pressure and vacuum suction. All the containers and the pipes were surrounded by the 37°C water jacket, thus all the superfusion experiments were performed at 37°C.

## **2.4 Measurement of SMA diameter**

The spiral modiolar artery was visualized through a microscope at 40X magnification. A black and white video camera (WV-1550, Panasonic) was connected to the inverted microscope (TE-300, Nikon). The microscope image was mixed with a time signal produced by the time code generator (Fast Forward Video). The images showed on the monitor (PVM-137, Sony) and recorded by a videotape recorder (AG-1960 Panasonic). The outer diameter of the SMA was monitored by a video-edge detector (Crescent Electronics). The video-edge detector affiliated with a computer program (AxoScope 10.2) and recorded digitized data about the diameter changes of SMA. All the digitized data was stored in ASCII format for later analysis and plotting (Origin 6.0).

After SMA being isolated and cut into segments, one segment was transferred into the superfusion chamber and filled with 1 mM  $\text{Ca}^{2+}$  solution. It was held in place by two blunted glass needles mounted on micromanipulators. After the segment was secure, it was superfused with 1 mM  $\text{Ca}^{2+}$  solution for 1 minute. To induce a constriction, the 1 mM  $\text{Ca}^{2+}$  valve is closed and the 10 mM  $\text{Ca}^{2+}$  valve is open and the SMA is superfused for 1 minute with 10 mM  $\text{Ca}^{2+}$  solution, which caused a constriction. This constriction was set to 100 %, and used as a control to compare to the constriction caused by ET-1 in the presence of drugs which we needed to test. After 1 minute of 10 mM  $\text{Ca}^{2+}$  was over, the valve was closed and the 1 mM  $\text{Ca}^{2+}$  valve was opened and the SMA was superfused for 1 minute with this solution. At 1.0 mM  $\text{Ca}^{2+}$  solution period, the SMA diameter quickly returned to its normal diameter. This process was repeated once again.

To determine whether the drug is an antagonist, the 1 mM Ca<sup>2+</sup> valve was closed and the drug valve was open and the SMA was superfused for 1 minute with the X μM (In Chapter 2.1 means the desired concentration of compound) solution of the drug. This step was performed to determine if the drug alone had any effect on the SMA. After this SMA being superfused for 1 or 2 minutes with the drug alone, the drug valve was closed and the SMA was superfused for 1 minute with the combination solution of X μM drug and 1 nM ET-1. If the drug was an antagonist, no constriction should be observed or the constriction can be smaller compared with the constriction caused by the 10 mM Ca<sup>2+</sup>.

## 2.5 The results and statistics

Next is a case as described above: compound TM-1 was tested as an example to illustrate.

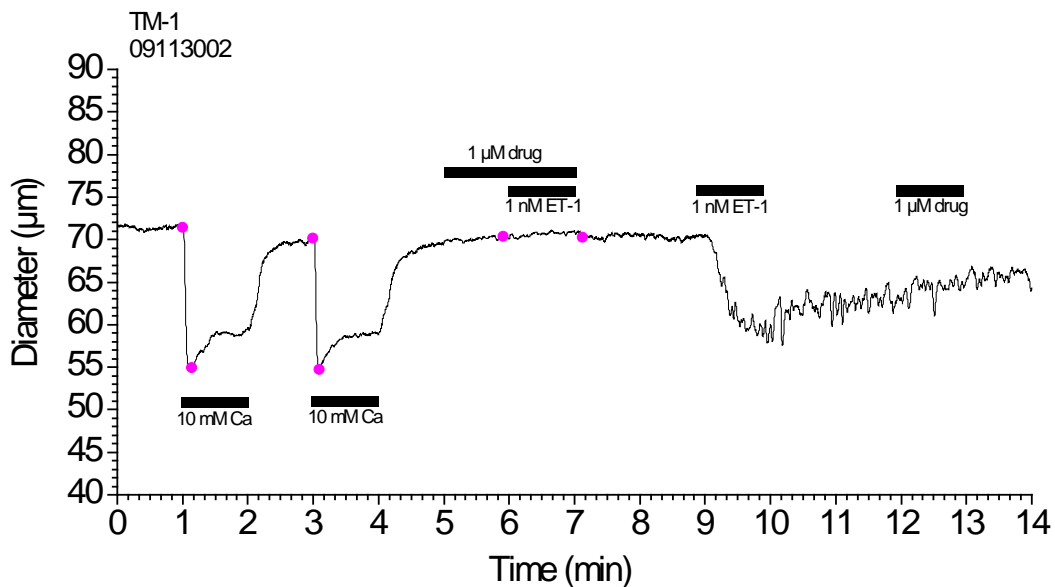


Figure 9. SMA diameter changes in superfusion (1.0 μM TM-1)  
All the SMA diameter changes were measured by software Origin 6.0.

From Figure 9 it is easy to read all superfusing changes: from 0~1 minute, 1 mM  $\text{Ca}^{2+}$  solution was superfused, the diameter of SMA didn't change. Because the cytosolic calcium concentration was the same as the 1mM  $\text{Ca}^{2+}$  solution and the other important cation concentrations are the same between the cytosolic solution and the solution around the SMA. From the 1<sup>st</sup> ~ 2<sup>nd</sup> minute, 10 mM  $\text{Ca}^{2+}$  solution was superfused and the SMA constricted immediately. In other words, the diameter of SMA decreased. Because the increasing of extracellular calcium concentration can cause the increasing of intracellular calcium concentration by getting through the calcium ion channels, and then it will result the series of physiological changes as described in chapter 1. From 2<sup>nd</sup> ~ 3<sup>rd</sup> minute, 1 mM  $\text{Ca}^{2+}$  solution was superfused again, the SMA diameter went back. From 3<sup>rd</sup> ~ 5<sup>th</sup> minute, The previous procedures were repeated by changing the 1 mM  $\text{Ca}^{2+}$  and 10 mM  $\text{Ca}^{2+}$  solution. SMA constrictions caused by the 10 mM  $\text{Ca}^{2+}$  were averaged twice and the average value is 15.96  $\mu\text{m}$ . This constriction was set to 100 %, and used as a control group to compare to the constriction caused by ET-1 in the presence of TM-1. From the 5<sup>th</sup> ~ 6<sup>th</sup> minute, the SMA was superfused with 1  $\mu\text{M}$  TM-1 and consequently the diameter of SMA has no change. That means 1  $\mu\text{M}$  TM-1 alone has no effect on the SMA. From the 6<sup>th</sup> ~ 7<sup>th</sup> minute, the SMA was superfused with the combination solution of 1  $\mu\text{M}$  TM-1 and 1 nM ET-1. There is still no significant change on SMA diameter. In other words, the constriction caused by 1 nM ET-1 in the presence of compound is 0  $\mu\text{m}$ . That means the 1  $\mu\text{M}$  TM-1 has antagonistic activity on 1 nM of ET-1. From 7<sup>th</sup> ~ 9<sup>th</sup> minute, we used 1 mM  $\text{Ca}^{2+}$  to wash away the ET-1 and TM-1. From 9<sup>th</sup> ~ 10<sup>th</sup> minute, the SMA constricted because of the superfusion of 1 nM ET-1. However, from the twelfth to thirteenth minute, the diameter of SMA went back a little and the trend is kind of slope shape. Actually, from the observation of monitor, the diameter of SMA didn't change during 10<sup>th</sup> ~ 13<sup>th</sup> minute. The slope trend at 10<sup>th</sup> ~ 13<sup>th</sup> minute was resulted from the fluctuation of video edge detector. Because video edge detector measure SMA diameter by differentiate the black and white boundary on the monitor. When the valves were switched to superfuse different solutions, the minor superfusion power difference and the alternation of superfusion direction can change the superfusion vector. Finally the position of SMA moved a little and the black spot on SMA may fall over video edge detector. Therefore, it is important to record all phenomenon observed on the monitor to avoid the error caused by the video edge detection fluctuation. The comprehensive judgment should based on the manually observation and the machine-record data.

Therefore, in this example, it is obviously to conclude that 1  $\mu\text{M}$  TM-1 can prevent the constriction caused by 1 nM ET-1, but it cannot recover the constriction caused by 1 nM ET-1. The constriction caused by 1 nM ET-1 in the presence of TM-1 is 0  $\mu\text{m}$ . Compared with the constricted averaged diameter value (15.96  $\mu\text{m}$ ) of SMA caused by the 10 mM  $\text{Ca}^{2+}$  solution, the percent of 1 nM ET-1 induced constriction in the presence of 1  $\mu\text{M}$  TM-1 is 0%.

However, more SMA segments need to be tested with the same method, thus the result will be more reliable.

It is also good to decrease the concentration of TM-1 drug and use the same method to record all SMA diameter changes caused by 10 mM  $\text{Ca}^{2+}$ , X  $\mu\text{M}$  (In Chapter 2.1 means the desired concentration of compound) TM-1 solution, combination solution of X  $\mu\text{M}$  drug and 1 nM ET-1, and 1 nM ET-1 respectively.

Next is another example to test TM-1's antagonistic ability.

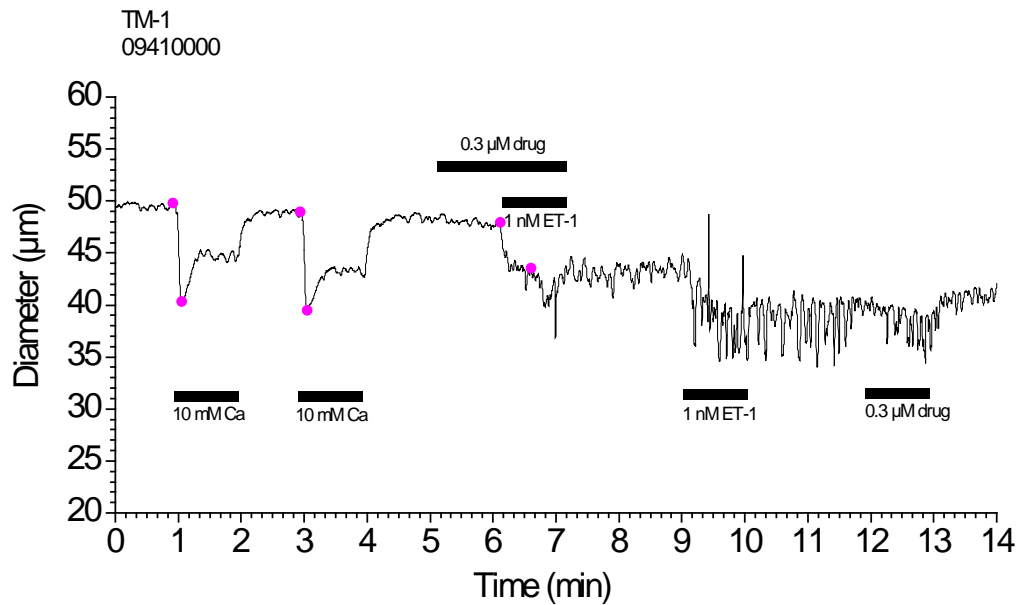


Figure 10. SMA diameter changes in superfusion (0.3  $\mu\text{M}$  TM-1)

In this case, the same method described in the last example was applied to test TM-1's antagonistic activity. The only difference is that SMA was superfused by 0.3  $\mu\text{M}$  TM-1 instead of 1  $\mu\text{M}$  TM-1 during 5<sup>th</sup> ~ 6<sup>th</sup> minute; 0.3  $\mu\text{M}$  drug and 1 nM ET-1 combination solution was superfused at 6 ~ 7 minute. As expected, the antagonistic function also decreased accompanied with the decrease concentration of TM-1 drug. In this case, the constriction caused by 1 nM ET-1 in the presence of TM-1 was 4.36  $\mu\text{m}$  while the constricted averaged diameter value of SMA caused by 10 mM  $\text{Ca}^{2+}$  solution was 9.48. Therefore, the percent of 1 nM ET-1 induced constriction in the presence of 0.3  $\mu\text{M}$  TM-1 is 45.99%.

The concentrations of TM-1 were decreased continually to test the antagonistic function. Next is the example for testing 0.1  $\mu\text{M}$  TM-1's antagonistic activity in the presence of 1 nM of ET-1.

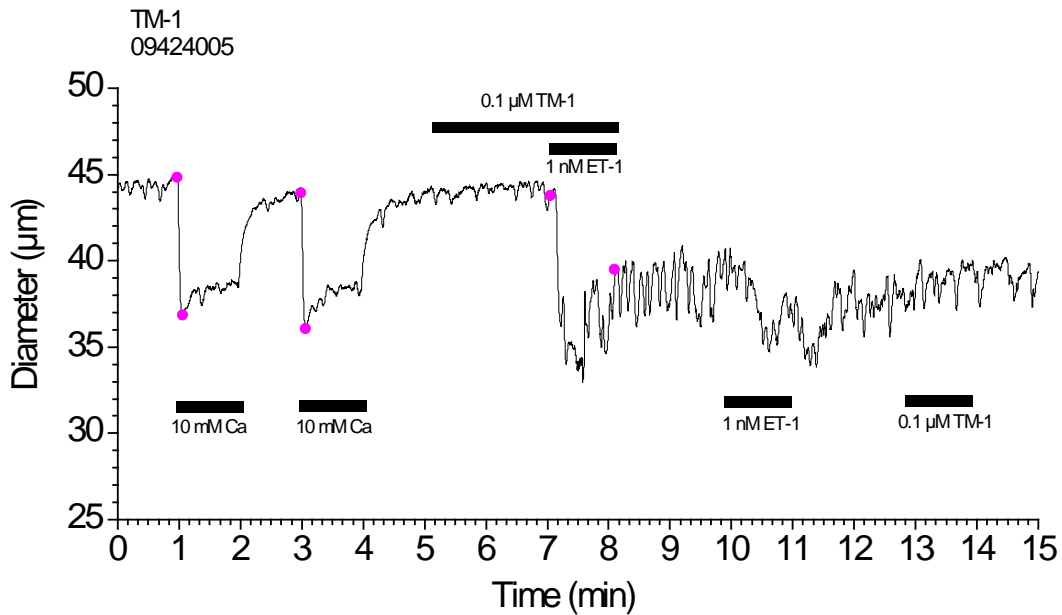


Figure 11. SMA diameter changes in superfusion (0.1  $\mu\text{M}$  TM-1)

In this case, the same method described in the last two examples was applied to test TM-1's antagonistic activity. The only difference is that SMA was superfused 0.1  $\mu\text{M}$  TM-1 instead of 1  $\mu\text{M}$  TM-1 during 5<sup>th</sup> ~ 6<sup>th</sup> minute; 0.1  $\mu\text{M}$  drug and 1 nM ET-1 combination solution was



superfused at 6 ~ 7 minute. As expected, the antagonistic function also decreased accompanied with the decrease concentration of TM-1 drug. The constriction caused by 1 nM ET-1 in the presence of TM-1 was 4.28  $\mu\text{m}$  while the constricted averaged diameter value of SMA caused by 10 mM  $\text{Ca}^{2+}$  solution was 7.93. Therefore, the percent of 1 nM ET-1 induced constriction in the presence of 0.3  $\mu\text{M}$  TM-1 is 53.97%.

TM-1's antagonistic function were tested at three different concentration, 0.1, 0.3 1.0  $\mu\text{M}$  respectively. At each concentration, several SMA segments were used to do the superfusion test. Then a table based on the data obtained.

Table 1. percentage of antagonistic activity of TM-1

entry	concentration of TM-1 ( $\mu\text{M}$ )	control constriction: Average of 10mM $\text{Ca}^{2+}$ constriction ( $\mu\text{m}$ )	constriction caused by 1 nM ET-1 in the presence of TM-1 ( $\mu\text{m}$ )	percentage of 1 nM ET-1 induced constriction in the presence of TM-1
1	0.1	6.86	4.11	59.91
2	0.1	4.29	2.85	66.43
3	0.1	7.93	4.28	53.97
4	0.1	4.23	2.36	55.79
5	0.1	4.22	2.40	56.87
6	0.1	9.11	4.63	50.82
7	0.3	9.48	4.36	45.99
8	0.3	6.99	3.45	49.36
9	0.3	7.23	4.13	57.12
10	0.3	11.08	2.38	21.48
11	0.3	9.72	2.84	29.22
12	0.3	5.58	1.73	31.00
13	1.0	18.77	0	0
14	1.0	15.96	0	0
15	1.0	7.20	0	0
16	1.0	4.46	1.19	26.68
17	1.0	7.00	0.39	5.57

The first column of the table from left is the entry number. The second column is the concentration of TM-1. There were six, six and five segments of SMA tested under 0.1, 0.3 and 1.0  $\mu\text{M}$  of TM-1 respectively. In order to obtain the percent of 1 nM ET-1 induced constriction in the presence of different concentrations of TM-1 drug. The constriction values which were caused by the 1 nM ET-1 in the presence of the compound were divided by the averaged constriction values caused by 10 mM  $\text{Ca}^{2+}$  solution.

To evaluate whether the other 5 (+)-myricic acid A intermediates have the ET-1 antagonistic function, the same method above was adopted to test them. Scheme 10 ~ Scheme 31 are the SMA diameter changes in superfusion of other compounds (TM-2, TM-3, TM-4, TM-5, TM-6 and (+)-myricic acid A) at different concentrations. Each compound should be tested at least three different concentrations and at least three SMA segments were tested under each certain concentration.

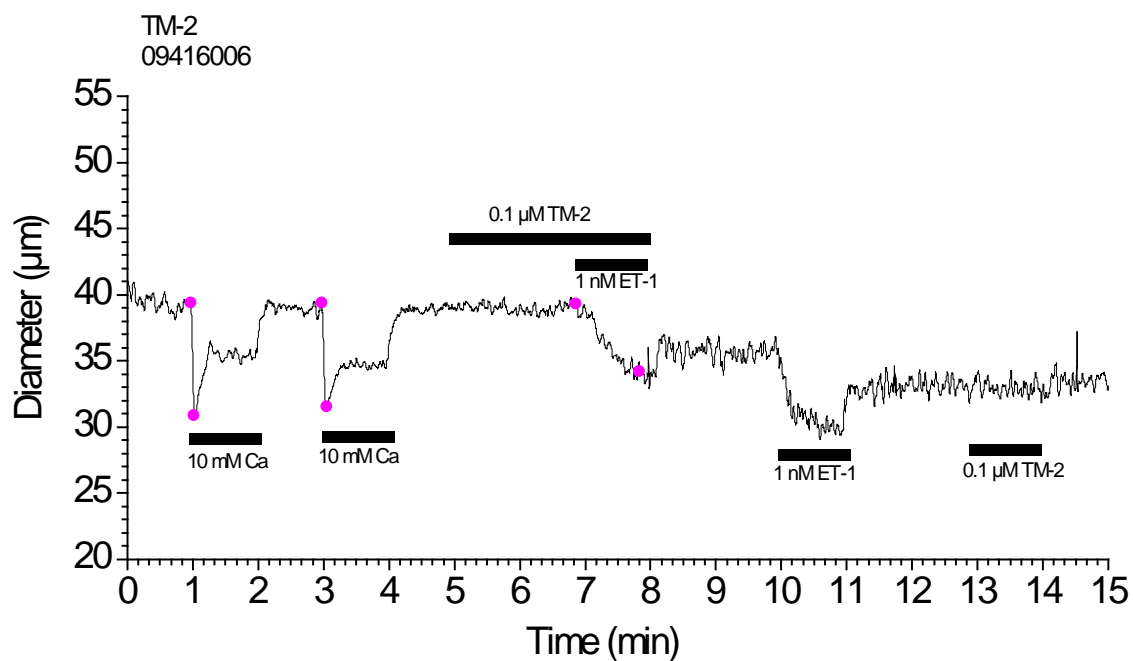


Figure 12. SMA diameter changes in superfusion (0.1  $\mu\text{M}$  TM-2)

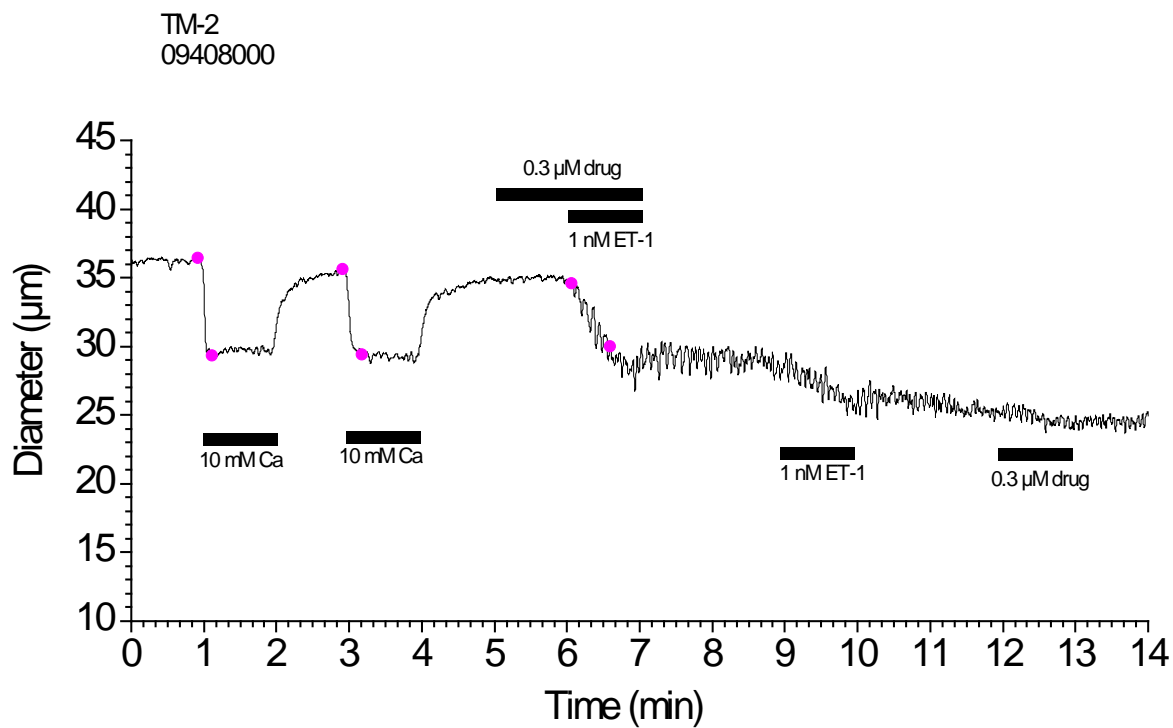


Figure 13. SMA diameter changes in superfusion (0.3 µM TM-2)

A09220000.abf  
3/17/2009 16:54

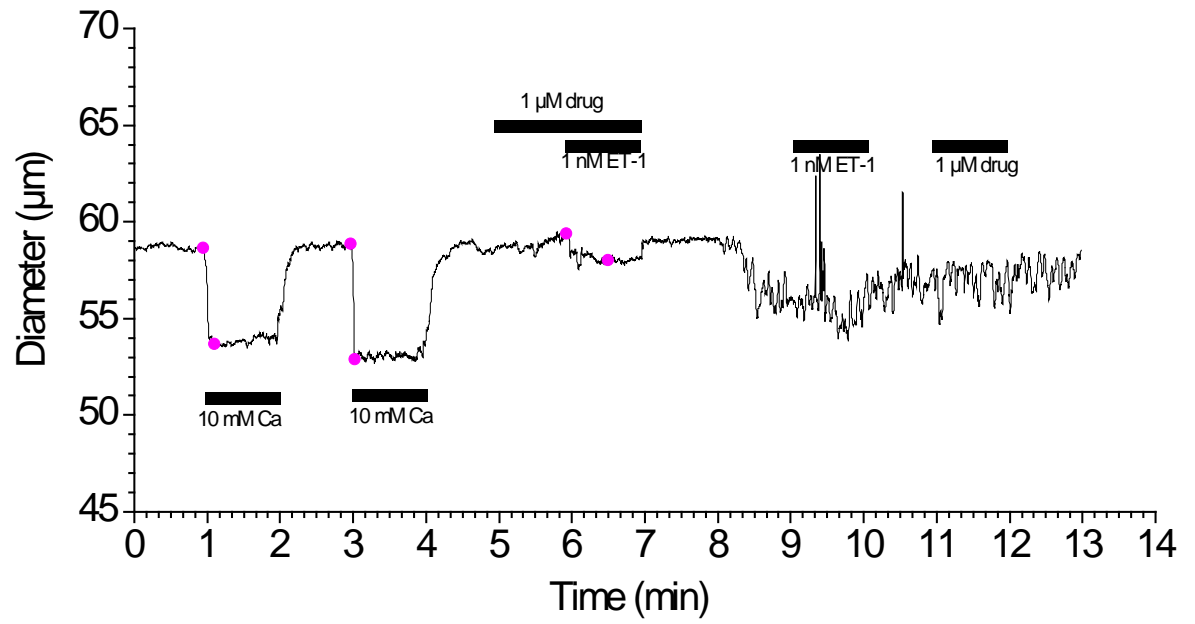


Figure 14. SMA diameter changes in superfusion (1.0 μM TM-2)

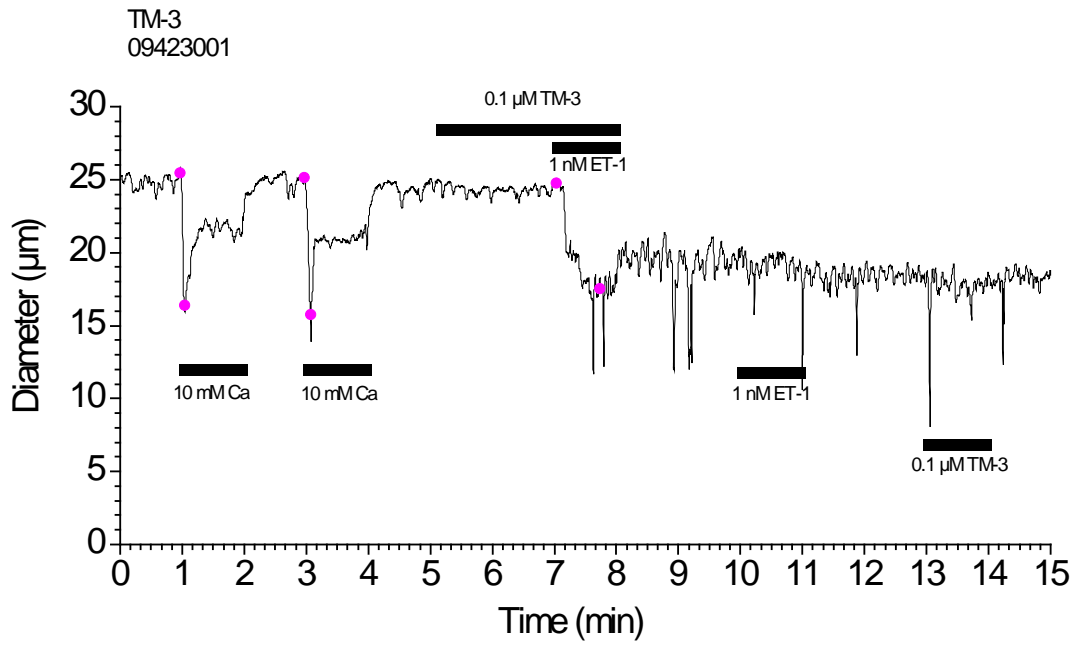


Figure 15. SMA diameter changes in superfusion (0.1 µM TM-3)

A09413002.abf  
4/13/2009 20:27

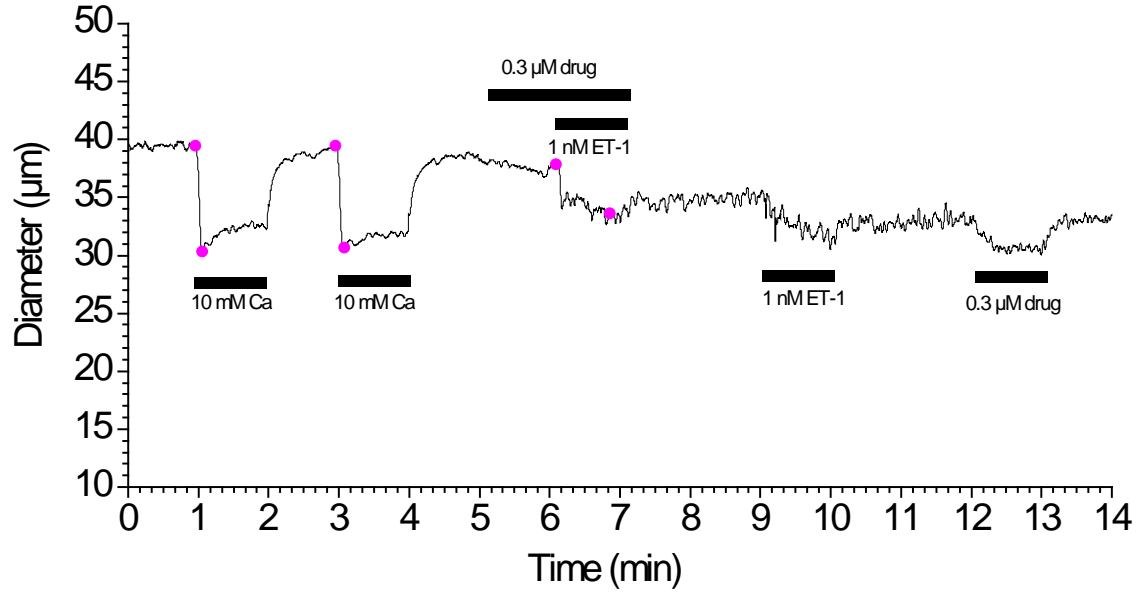


Figure 16. SMA diameter changes in superfusion (0.3 μM TM-3)

A09d03014.abf  
12/6/2009 21:11

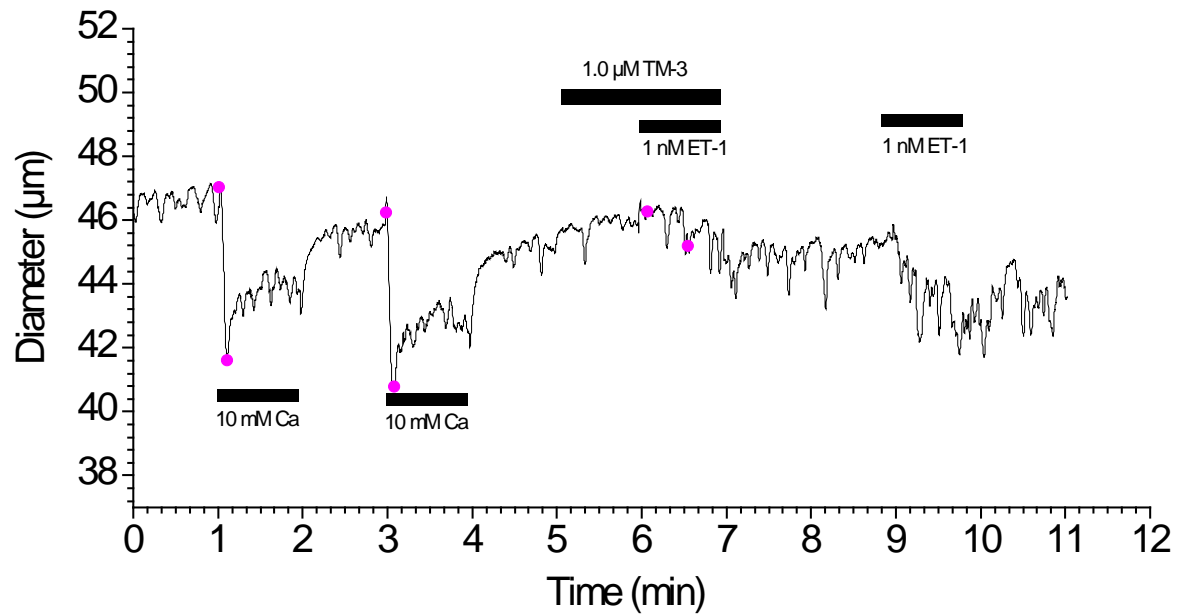


Figure 17. SMA diameter changes in superfusion (1.0 μM TM-3)

A09413001.abf  
4/13/2009 20:22

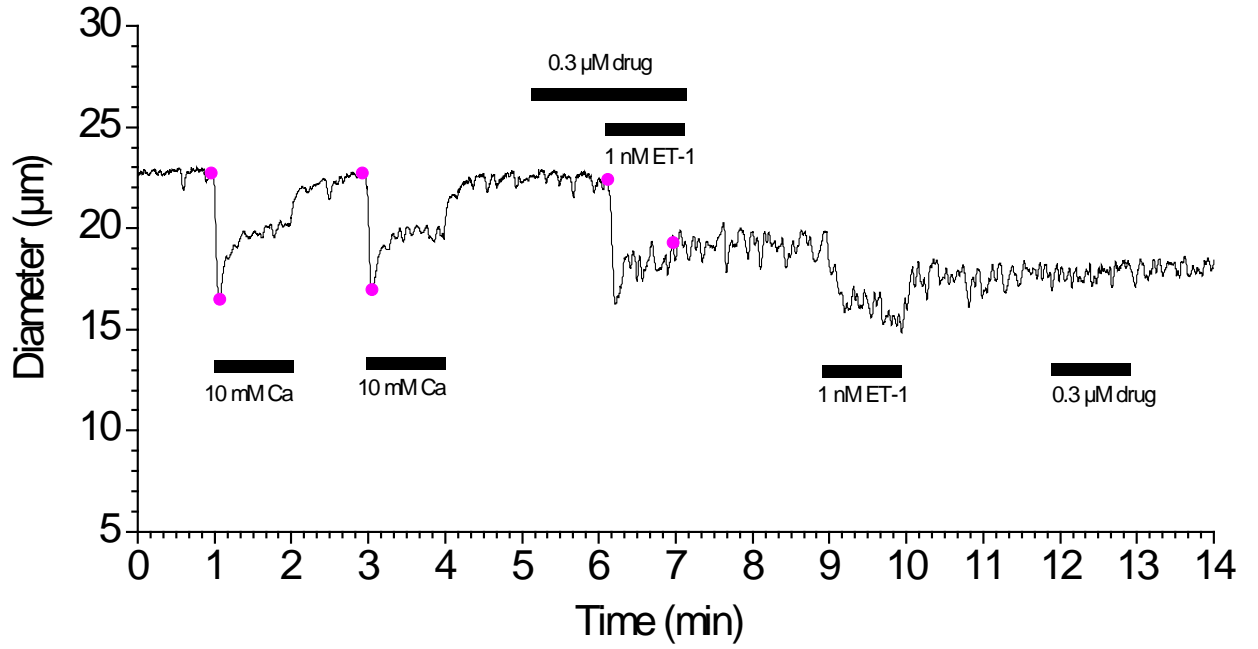


Figure 18. SMA diameter changes in superfusion (0.3 μM TM-4)



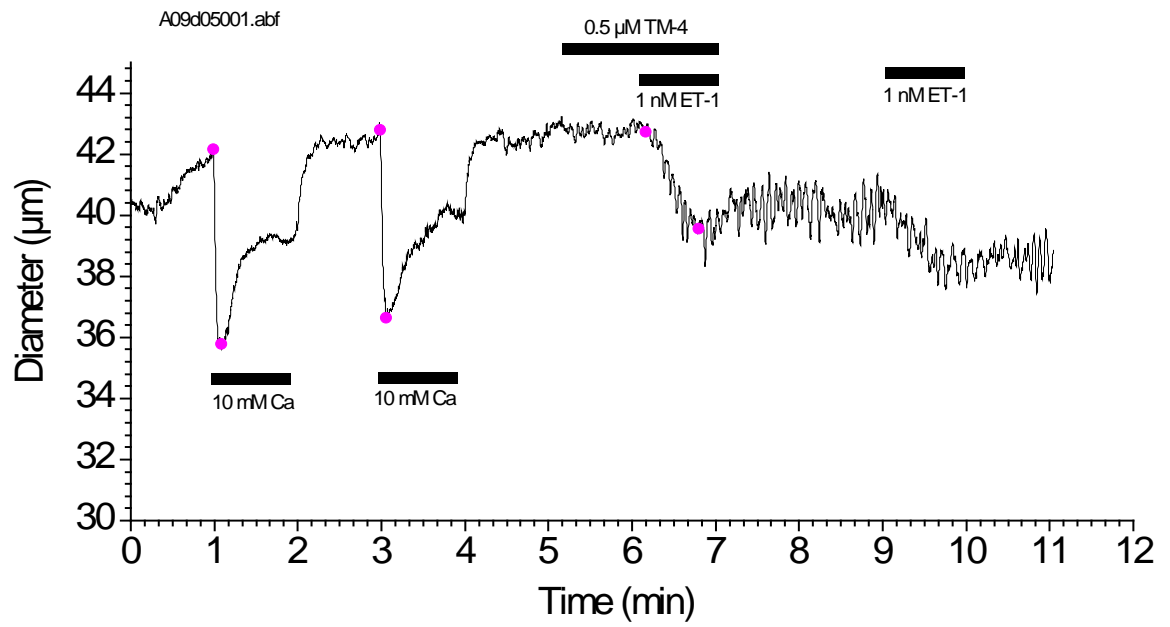


Figure 19. SMA diameter changes in superfusion (0.5  $\mu\text{M}$  TM-4)

A09d05005.abf

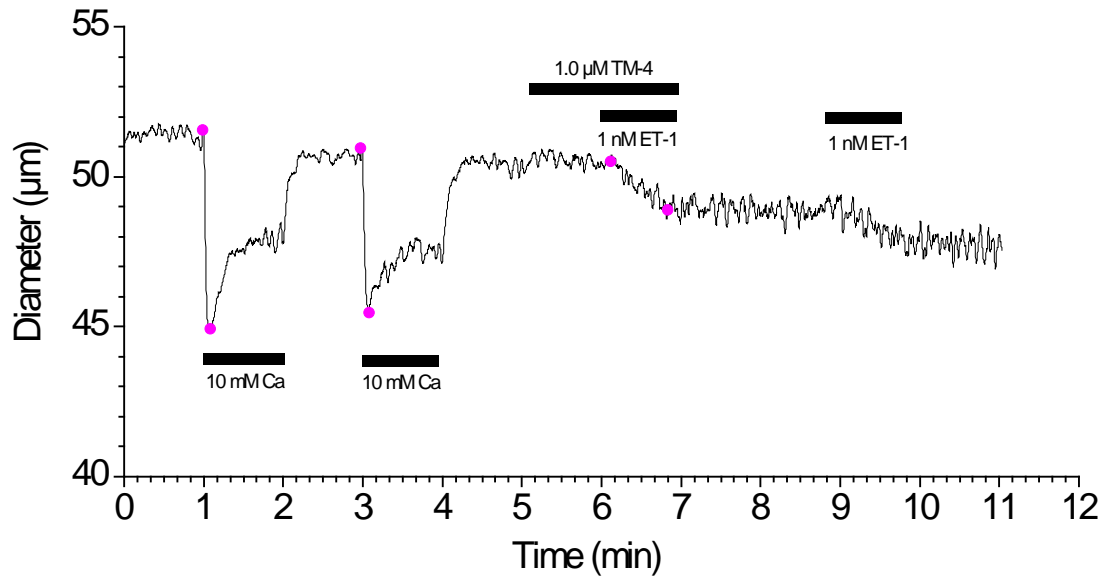


Figure 20. SMA diameter changes in superfusion (1.0  $\mu\text{M}$  TM-4)

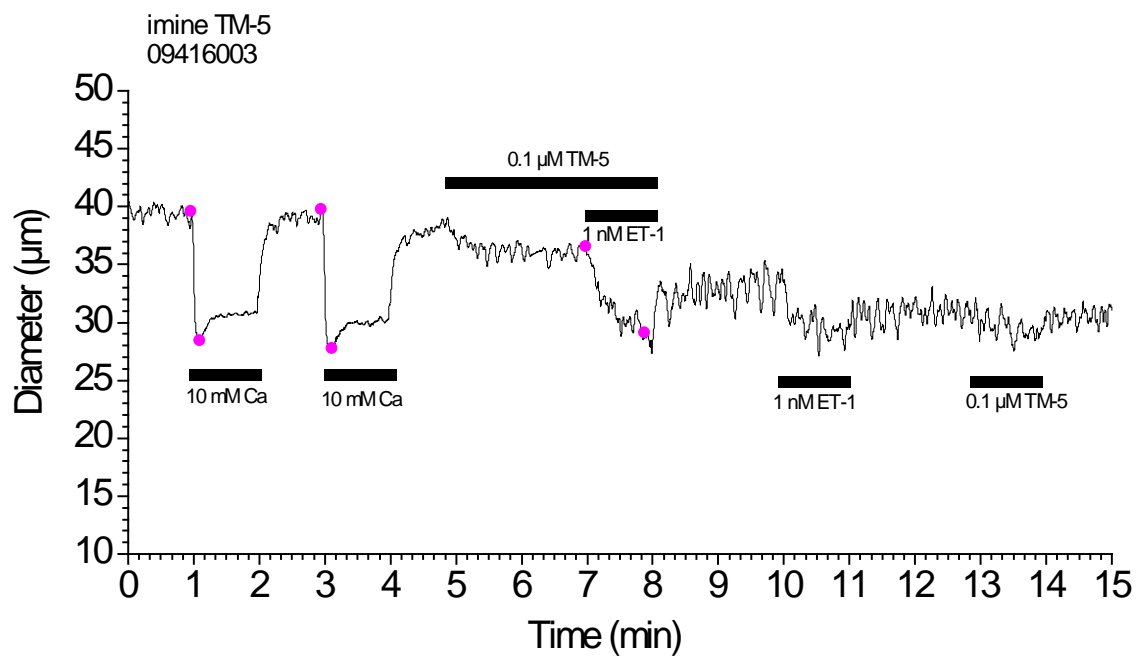


Figure 21. SMA diameter changes in superfusion (0.1  $\mu\text{M}$  TM-5)

A09507001.abf

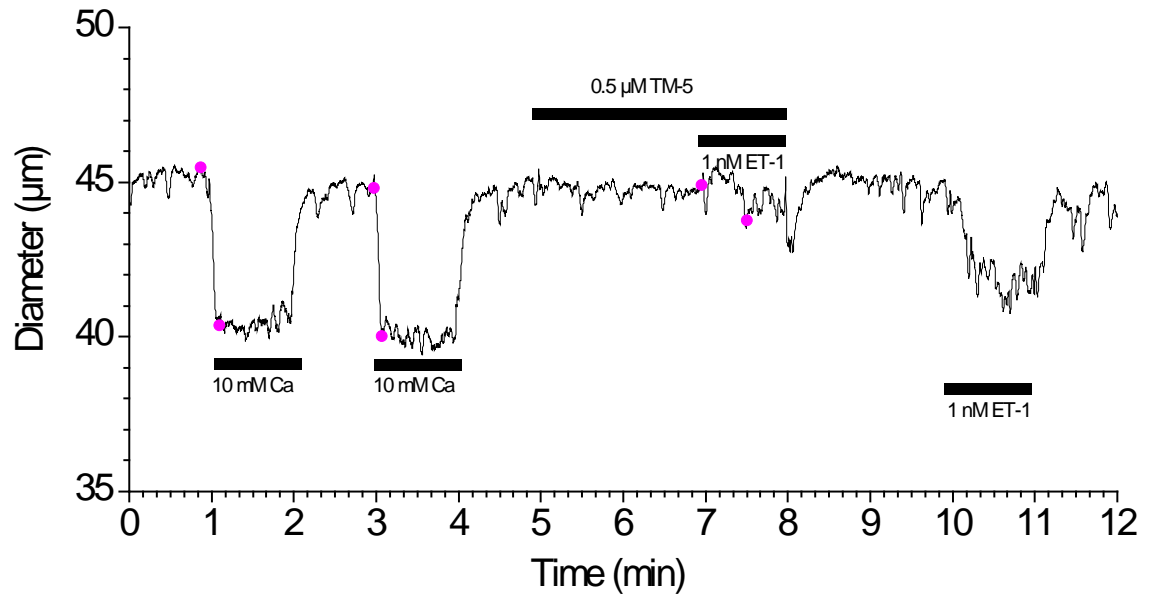


Figure 22. SMA diameter changes in superfusion (0.5 μM TM-5)

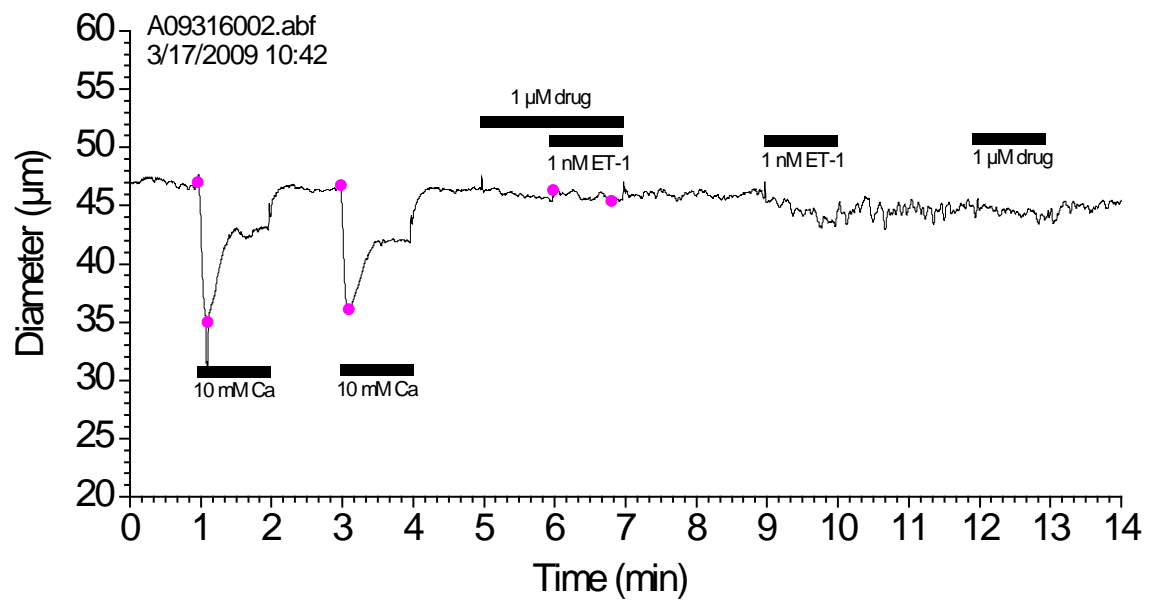


Figure 23. SMA diameter changes in superfusion (1.0  $\mu\text{M}$  TM-5)

A09408001.abf  
4/9/2009 16:45

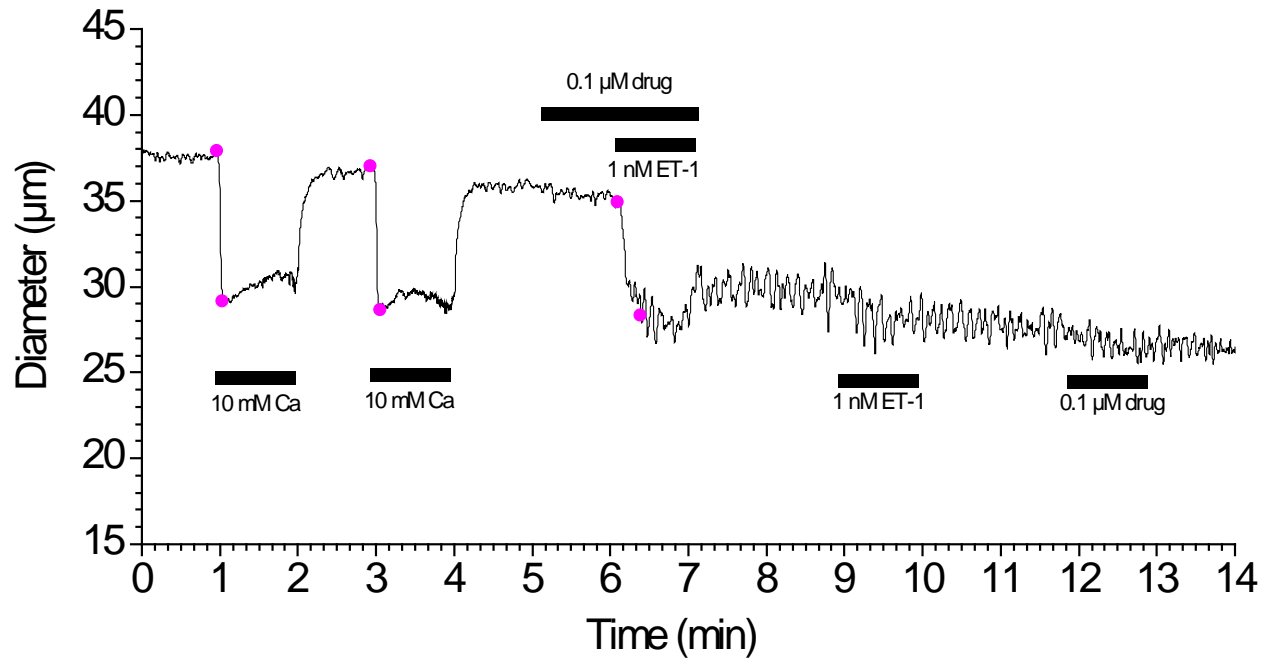


Figure 24. SMA diameter changes in superfusion (0.1 μM TM-6)

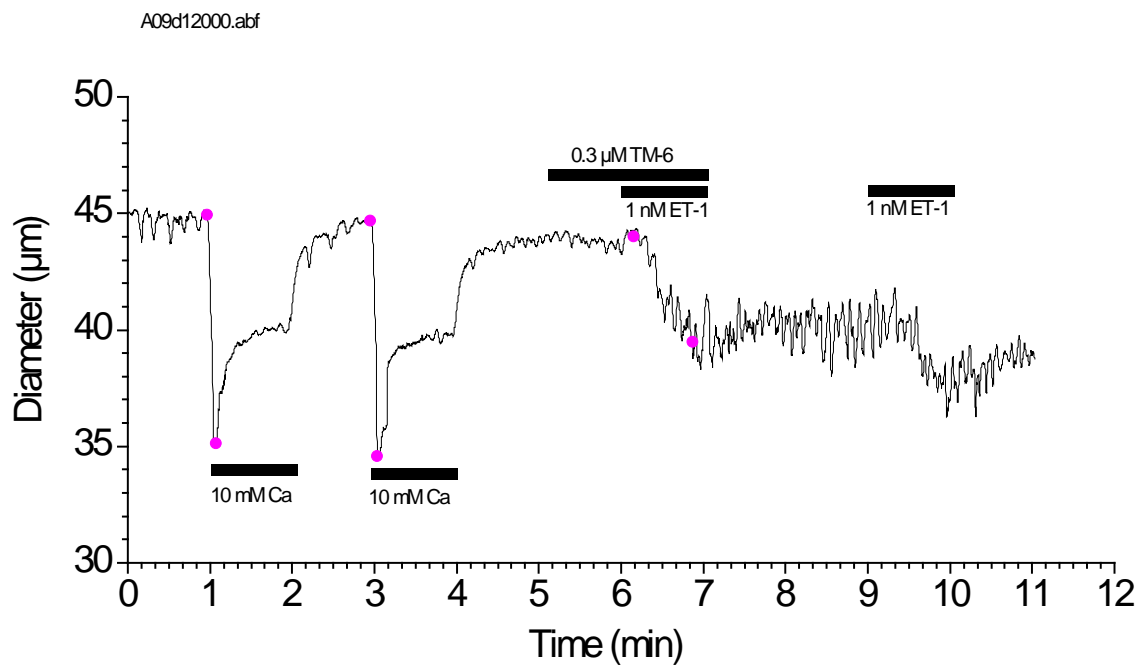


Figure 25. SMA diameter changes in superfusion (0.3  $\mu\text{M}$  TM-6)

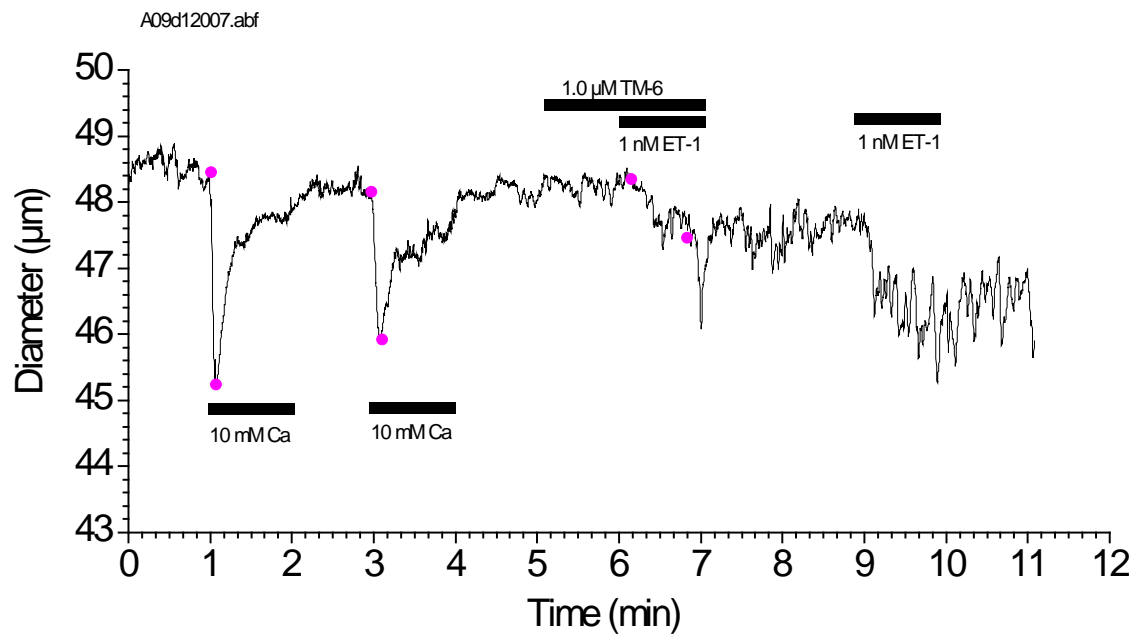


Figure 26. SMA diameter changes in superfusion (1.0 µM TM-6)



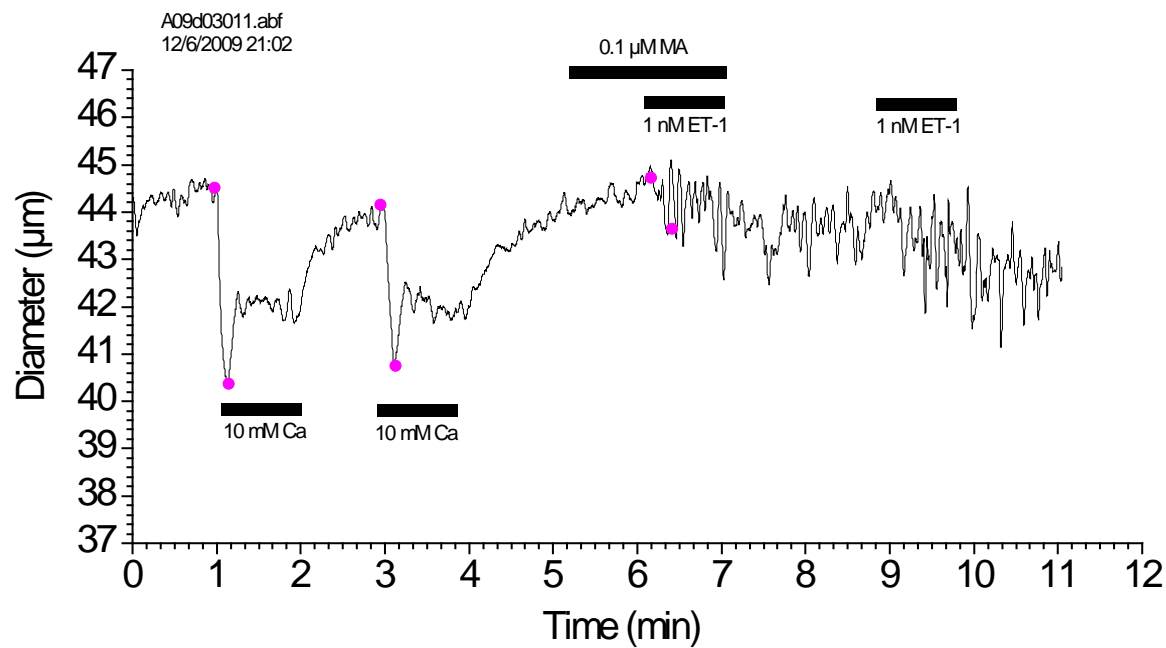


Figure 27. SMA diameter changes in superfusion (0.1 µM (+)-myriceric acid A)

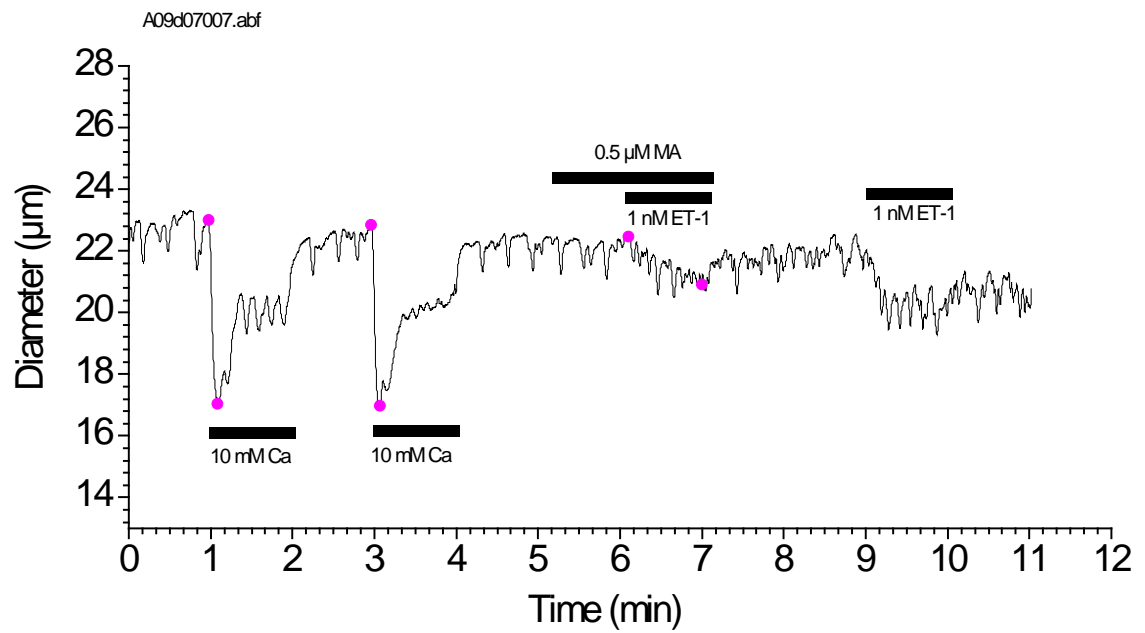


Figure 28. SMA diameter changes in superfusion (0.5 µM (+)-myriceric acid A)

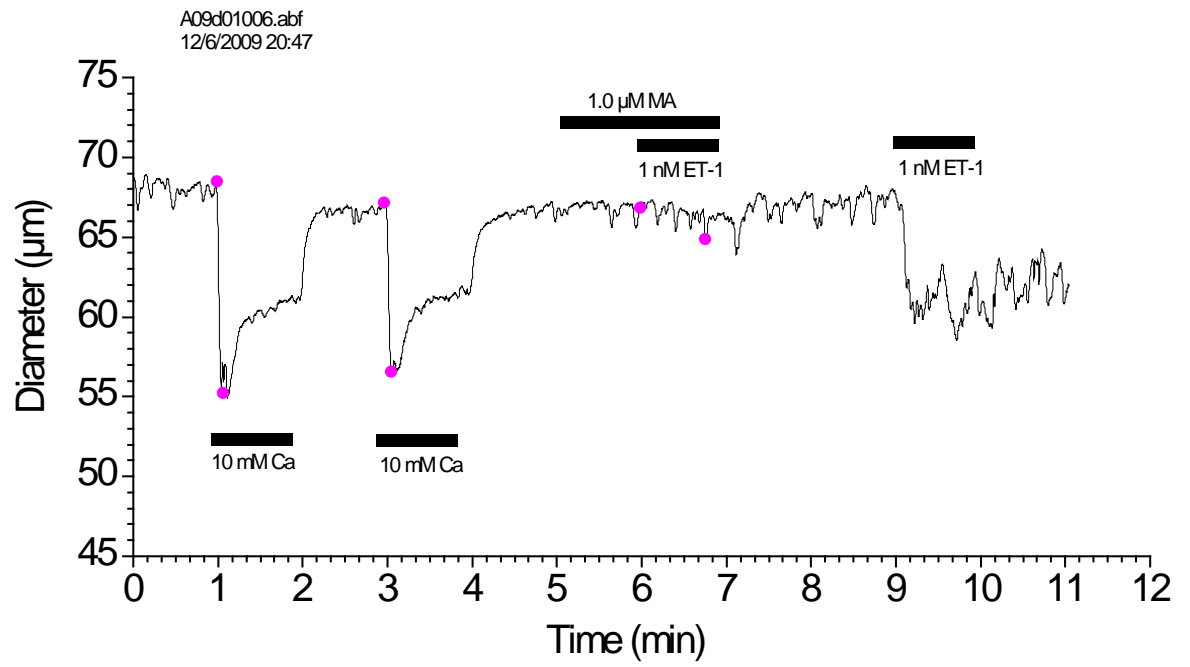


Figure 29. SMA diameter changes in superfusion (1.0  $\mu\text{M}$  (+)-myriceric acid A)

Finally, data in the other 6 tables were obtained. Next table is about TM-2 antagonistic activity:

Table 2. percentage of antagonistic activity of TM-2

entry	concentration of TM-2 ( $\mu\text{M}$ )	control constriction: Average of 10mM $\text{Ca}^{2+}$ constriction ( $\mu\text{m}$ )	constriction caused by 1 nM ET-1 in the presence of TM-2 ( $\mu\text{m}$ )	percentage of 1 nM ET-1 induced constriction in the presence of TM-2
1	0.1	8.17	5.11	62.55
2	0.1	12.47	10.86	87.09
3	0.1	8.45	6.70	79.29
4	0.1	5.32	5.07	95.30
5	0.3	5.85	2.80	47.86
6	0.3	6.70	4.60	68.66
7	0.3	3.38	1.80	53.25
8	0.3	4.10	2.10	51.22
9	0.3	6.98	4.18	59.89
10	1.0	5.48	1.35	24.64
11	1.0	5.24	0	0
12	1.0	11.81	2.54	21.51
13	1.0	7.22	1.59	22.02
14	1.0	3.90	0.95	24.36

From this table, it shows that TM-2 also has ET-1 antagonistic function. When the concentration of TM-2 was 1.0  $\mu\text{M}$ , it had the greatest ET-1 blocking function compared with the other 2 concentrations. The percent of 1 nM ET-1 induced constriction in the presence of 1.0  $\mu\text{M}$  TM-2 is less than thirty percent. As the decreased concentration of TM-2 tested, the blocking function was also decreased. It is quite similar with TM-1.

Next are TM-3, TM-4, TM-5 and TM-6 antagonistic activity tables:

Table 3. percentage of antagonistic activity of TM-3

entry	concentration of TM-3 ( $\mu\text{M}$ )	control constriction: Average of 10mM $\text{Ca}^{2+}$ constriction ( $\mu\text{m}$ )	constriction caused by 1 nM ET-1 in the presence of TM-3 ( $\mu\text{m}$ )	percentage of 1 nM ET-1 induced constriction in the presence of TM-3
1	0.1	9.24	7.24	78.35
2	0.1	5.49	2.75	50.09
3	0.1	6.54	2.92	44.65
4	0.1	7.16	4.84	67.60
5	0.1	7.56	5.35	70.77
6	0.3	8.97	4.19	46.71
7	0.3	9.50	3.36	35.37
8	0.3	6.42	3.22	50.16
9	0.3	4.85	2.78	57.32
10	1.0	12.87	2.96	23.00
11	1.0	10.45	2.27	21.72
12	1.0	5.12	1.01	19.73
13	1.0	5.45	1.08	19.82
14	1.0	7.95	0.44	5.53

Table 4. percentage of antagonistic activity of TM-4

entry	concentration of TM-4 (μM)	control constriction: Average of 10mM Ca <sup>2+</sup> constriction (μm)	constriction caused by 1 nM ET-1 in the presence of TM-4 (μm)	percentage of 1 nM ET-1 induced constriction in the presence of TM-4
1	0.3	8.85	4.36	49.27
2	0.3	6.00	3.12	52.00
3	0.3	10.10	6.08	60.20
4	0.3	7.06	4.25	60.20
5	0.3	5.46	3.04	55.68
6	0.5	7.33	3.65	49.80
7	0.5	6.59	2.50	37.94
8	0.5	11.05	4.38	39.64
9	0.5	6.27	3.17	50.56
10	0.5	6.88	3.83	55.67
11	1.0	6.61	0.66	9.98
12	1.0	7.94	2.22	27.96
13	1.0	9.57	3.34	34.90
14	1.0	3.88	0.91	23.45
15	1.0	6.07	1.60	26.36
16	1.0	8.20	1.92	23.41
17	1.0	8.17	2.28	27.91

Table 5. percentage of antagonistic activity of TM-5

entry	concentration of TM-5 (μM)	control constriction: Average of 10mM Ca <sup>2+</sup> constriction (μm)	constriction caused by 1 nM ET-1 in the presence of TM-5 (μm)	percentage of 1 nM ET-1 induced constriction in the presence of TM-5
1	0.1	11.60	7.49	64.57
2	0.1	10.24	4.87	47.56
3	0.1	5.23	2.22	42.45
4	0.1	6.19	2.56	41.36
5	0.1	9.45	3.91	41.38
6	0.3	6.96	1.82	26.15
7	0.3	6.90	3.10	44.93
8	0.3	10.75	3.40	31.63
9	0.3	15.91	4.90	30.80
10	0.3	6.36	1.75	27.52
11	0.5	8.07	1.38	17.10
12	0.5	10.25	1.23	12.00
13	0.5	4.95	1.14	23.03
14	1.0	4.05	0.65	16.05
15	1.0	6.55	0.66	10.08
16	1.0	11.37	0.98	8.62
17	1.0	5.96	0	0
18	1.0	4.43	0	0

Table 6. percentage of antagonistic activity of TM-6

entry	concentration of TM-6 (μM)	control constriction: Average of 10mM Ca <sup>2+</sup> constriction (μm)	constriction caused by 1 nM ET-1 in the presence of TM-6 (μm)	percentage of 1 nM ET-1 induced constriction in the presence of TM-6
1	0.1	8.59	6.61	76.95
2	0.1	5.47	3.62	66.18
3	0.1	3.84	1.91	49.74
4	0.1	2.99	1.49	49.83
5	0.3	8.46	2.93	34.63
6	0.3	9.96	4.53	45.48
7	0.3	5.86	2.22	37.88
8	0.3	11.76	3.86	32.82
9	0.3	4.67	1.90	40.69
10	1.0	9.09	2.11	23.21
11	1.0	12.63	5.61	44.42
12	1.0	3.95	1.51	38.23
13	1.0	5.62	0.75	13.35
14	1.0	2.73	0.88	32.23

It is quite exciting that all the (+)-myriceric acid A intermediates have ET-1 blocking function. To evaluate which compound has a stronger blocking function, (+)-myriceric acid A was tested and the statistic table was concluded below.



Table 7. percentage of antagonistic activity of (+)-myriceric acid A

entry	concentration of (+)-myriceric acid A ( $\mu\text{M}$ )	control constriction: Average of 10mM $\text{Ca}^{2+}$ constriction ( $\mu\text{m}$ )	constriction caused by 1 nM ET-1 in the presence of (+)-myriceric acid A ( $\mu\text{m}$ )	percentage of 1 nM ET-1 induced constriction in the presence of (+)-myriceric acid A
1	0.1	5.92	2.22	37.50
2	0.1	6.54	2.09	31.96
3	0.1	3.78	1.06	28.04
4	0.1	6.07	2.03	33.44
5	0.1	6.25	1.83	29.28
6	0.5	7.97	2.22	27.85
7	0.5	10.34	1.59	15.38
8	0.5	8.57	2.22	25.90
9	0.5	8.29	1.21	14.60
10	0.5	5.92	1.55	26.18
11	1.0	21.65	3.56	16.44
12	1.0	11.94	1.97	16.50
13	1.0	5.27	0.74	14.04
14	1.0	6.05	0.94	15.54
15	1.0	2.50	0.40	16.00

## 2.6 Pharmacological analysis

In order to compare the antagonistic potency of (+)-myriceric acid A and its 6 different intermediate drugs, there were two relationships between concentration of compound and the percentage of 1 nM ET-1 induced constriction in the presence of compound proposed, linear and curve relationships. In the curve relationship, all the data in the above tables were normalized to the maximal increase in intracellular calcium and the maximal vasoconstriction induced by an elevation of the extracellular  $\text{Ca}^{2+}$  concentration from 1 mM to 10 mM  $\text{Ca}^{2+}$ . Normalized data were fitted with the equation:  $\mathbf{E} = \mathbf{Base} + \{(\mathbf{E}_{\text{maximal}} - \mathbf{Base}) \times [\mathbf{D}]^h / \mathbf{EC}_{50}^h + [\mathbf{D}]^h\}$  (**equation 3**)<sup>34</sup>

The theory for applying **equation 3** is briefly introduced below: If the drug needs to bind with receptor, an equilibrium equation is established:  $[\mathbf{R}] + [\mathbf{D}] \leftrightarrow [\mathbf{R} - \mathbf{D}]$  ([R] represents free receptor concentration, [D] represents drug concentration and [R-D] represents drug-receptor complex concentration). Based on the Law of Mass Action, **equation 4** is obtained:  $[\mathbf{R}] \times [\mathbf{D}] / [\mathbf{R} - \mathbf{D}] = \mathbf{K}_D$  (**equation 4**,  $\mathbf{K}_D$  is the equilibrium dissociation constant). Meanwhile,  $[\mathbf{R}] = [\mathbf{R}]_{\text{total}} - [\mathbf{R} - \mathbf{D}]$  (**equation 5**).

Substitute **equation 5** into **equation 4**  $\rightarrow [\mathbf{R} - \mathbf{D}] = ([\mathbf{R}]_{\text{total}} \times [\mathbf{D}]) / ([\mathbf{D}] + \mathbf{K}_D)$  (**equation 6**).

If the drug effect is proportional to [R-D] and k is the proportional constant, **equation 7** is obtained:  $\mathbf{E} = \mathbf{k} \times [\mathbf{R} - \mathbf{D}]$  (**equation 7**, E is the drug effect).

Therefore,  $\mathbf{E}_{\text{maximal}} = \mathbf{k} \times [\mathbf{R} - \mathbf{D}]_{\text{maximal}} = \mathbf{k} \times [\mathbf{R}]_{\text{total}}$  (**equation 8**)

Substitute **equation 7** and **equation 8** into **equation 6**, **equation 9** is obtained:

$$\mathbf{E} = \mathbf{E}_{\text{maximal}} \times [\mathbf{D}] / ([\mathbf{D}] + \mathbf{K}_D) \quad (\text{equation 9})$$

If [D] is equal to  $\text{EC}_{50}$  (antagonist concentration that induces a half maximal effect), **equation 9**  $= 0.5 \times \mathbf{E}_{\text{maximal}} \rightarrow 0.5 = [\mathbf{D}] / ([\mathbf{D}] + \mathbf{K}_D) \rightarrow [\mathbf{D}] = \mathbf{K}_D \rightarrow \mathbf{K}_D = \text{EC}_{50}$

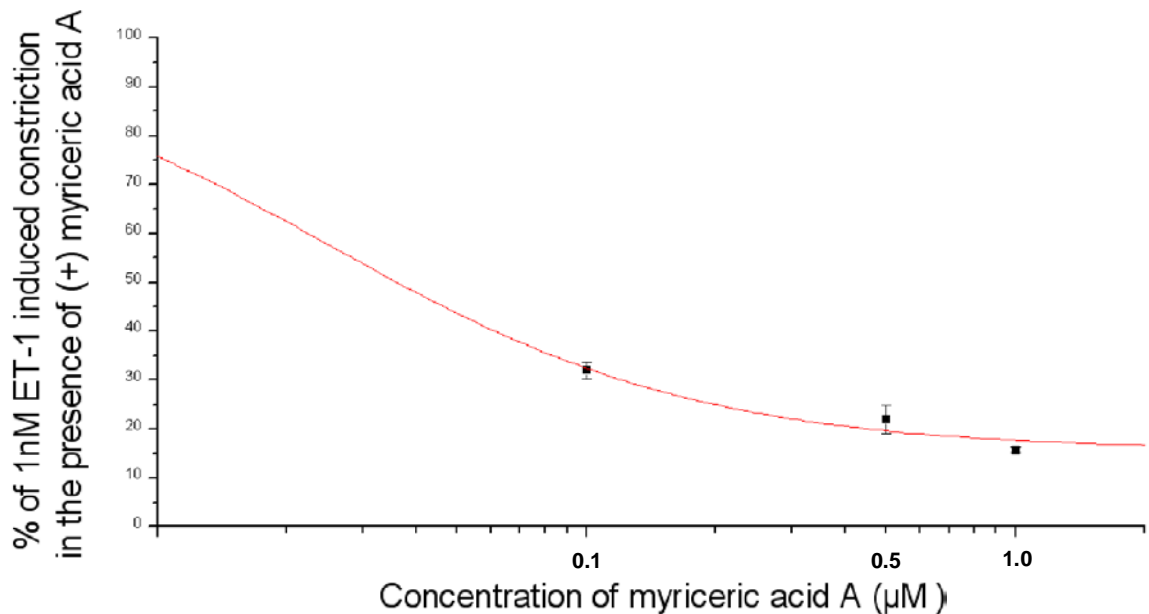
Substitute  $\text{EC}_{50} = \mathbf{K}_D$  into **equation 9**  $\rightarrow \mathbf{E} = \mathbf{E}_{\text{maximal}} \times [\mathbf{D}] / ([\mathbf{D}] + \text{EC}_{50})$  (**equation 10**)

If [D] is logarithm value, the relationship between E and [D] is sigmoid. The Hill coefficient is introduced in **equation 9** to give the largest absolute value of the slope of the curve. Moreover, because the potential maximum drug effect threshold may exist, the **Base** (the value of E which is infinitely close the horizontal axial) parameter is introduced in **equation 10**. Finally, the **equation 3** is obtained:  $\mathbf{E} = \mathbf{Base} + \{(\mathbf{E}_{\text{maximal}} - \mathbf{Base}) \times [\mathbf{D}]^h / \text{EC}_{50}^h + [\mathbf{D}]^h\}$ , this is

still sigmoid curve equation. **Equation 10** is widely used when people plot the non-linear relationship between drug dose and drug effect when it involve receptors. In this bioassay, E is the relative constriction (%),  $EC_{50}$  is the antagonist concentration that induced a half maximal effect.  $E_{\text{maximal}}$  is the maximal constriction, [D] is the concentration of agonist, h defines the slope and the Base means the value of E which is infinitely close the horizontal axial. All the data were presented as mean  $\pm$  sem. The parameters and dose-respond curves were obtained by using software Origin 6.0.

Next is the dose-respond curve of (+)-myriceric acid A:

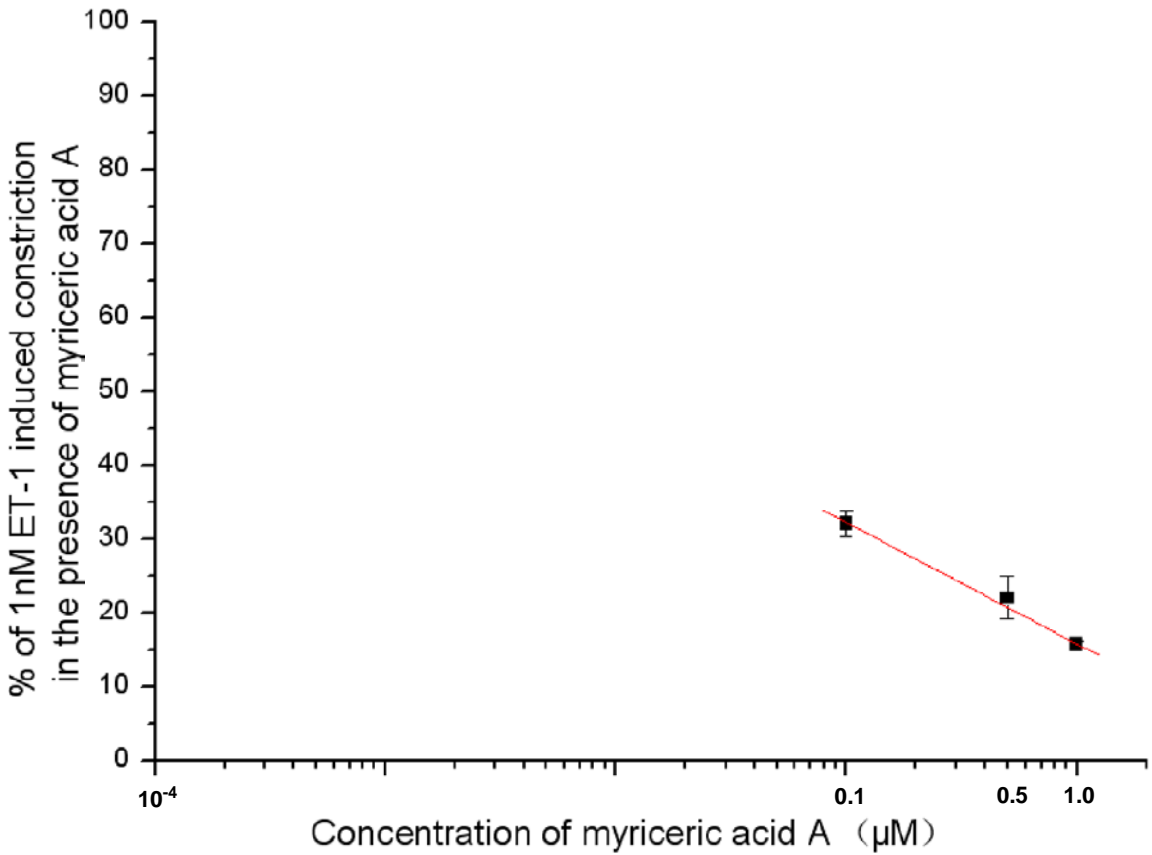
Graph 1. Percentage of 1 nM ET-1 induced constriction in the presence of (+)-myriceric acid A  
**Versus** concentration of (+)-myriceric acid A (curve)



The horizontal axial is the concentration of (+)-myriceric acid A based on the logarithm value. The vertical axial is the constriction value which was caused by the 1 nM ET-1 in the presence of (+)-myriceric acid A divided by the averaged constriction value caused by elevated 10 mM  $\text{Ca}^{2+}$  solution. All the data is from the table 7.

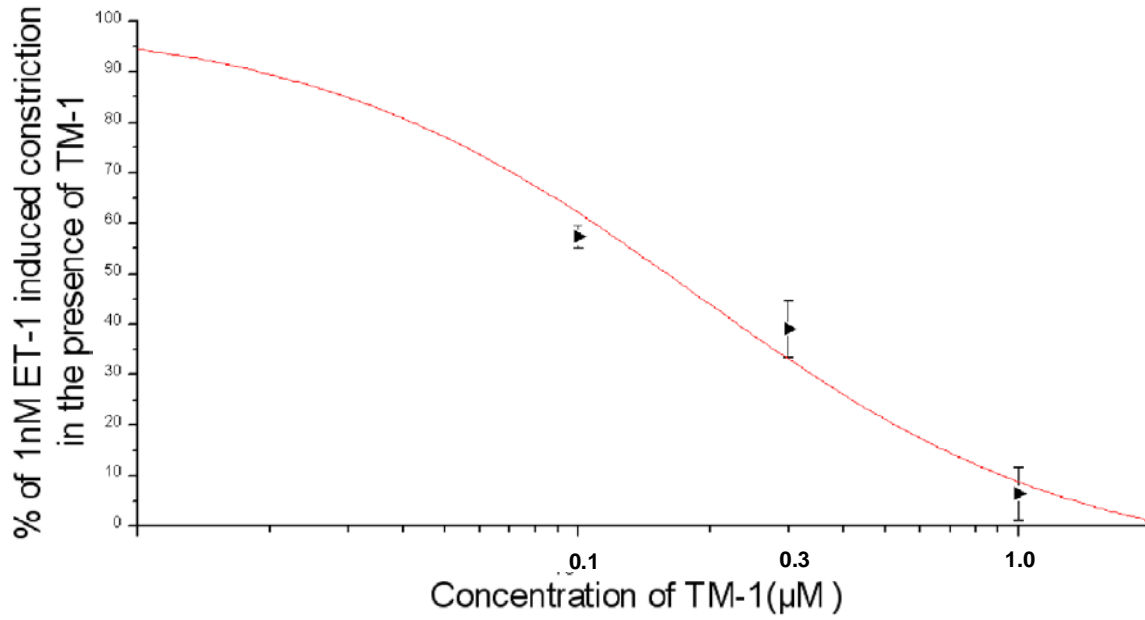
In the linear relationship, the horizontal axial is the concentration of (+)-myriceric acid A based on the logarithm value. The vertical axial is also the constriction value which was caused by the 1 nM ET-1 in the presence of (+)-myriceric acid A divided by the averaged constriction value caused by elevated 10 mM  $\text{Ca}^{2+}$  solution. (Graph 2)

Graph 2. Percentage of 1 nM ET-1 induced constriction in the presence of (+)-myriceric acid A  
**Versus** concentration of (+)-myriceric acid A (linear)

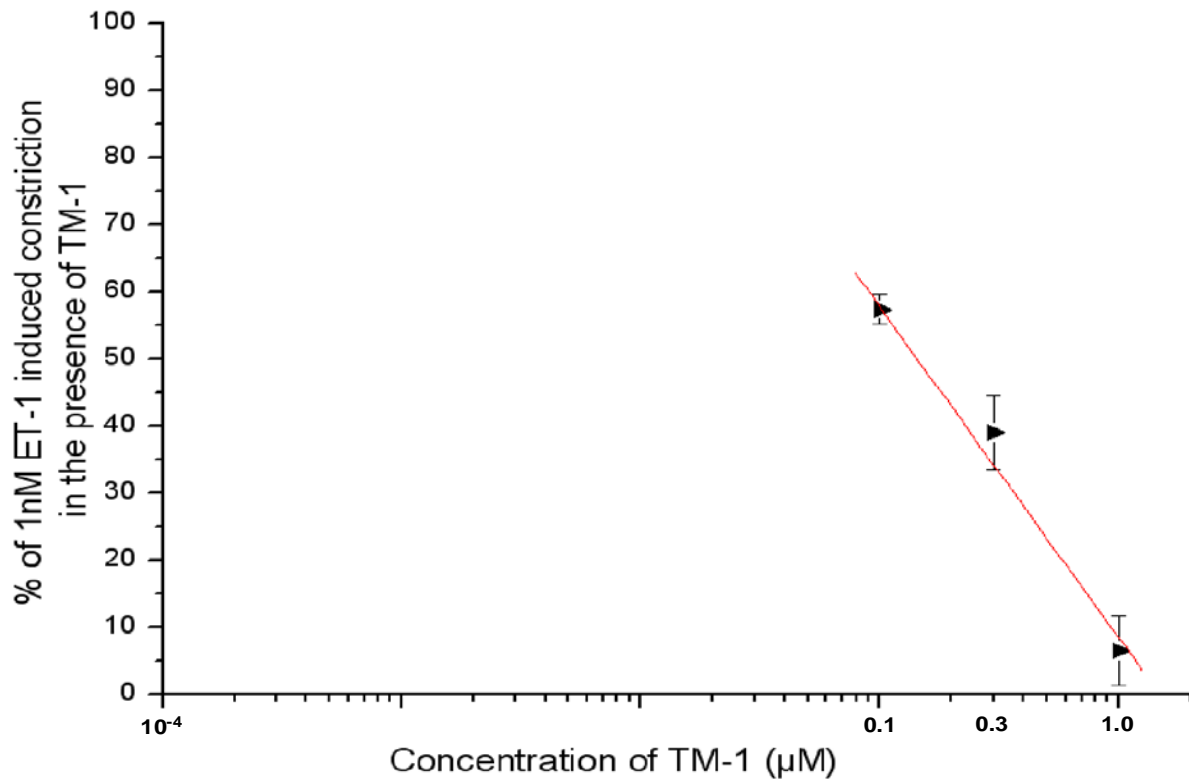


Similar graphs (curve and linear) were plotted based on the previous data showed in the Table 1 ~ Table 6

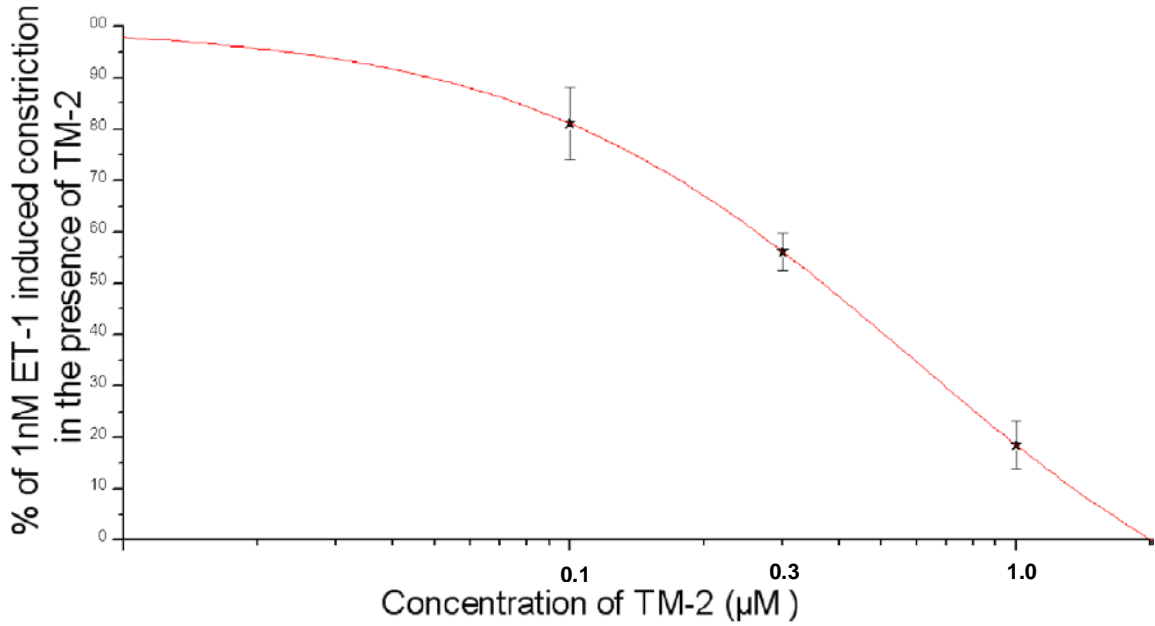
Graph 3. Percentage of 1 nM ET-1 induced constriction in the presence of TM-1 **Versus** concentration of TM-1 (curve)



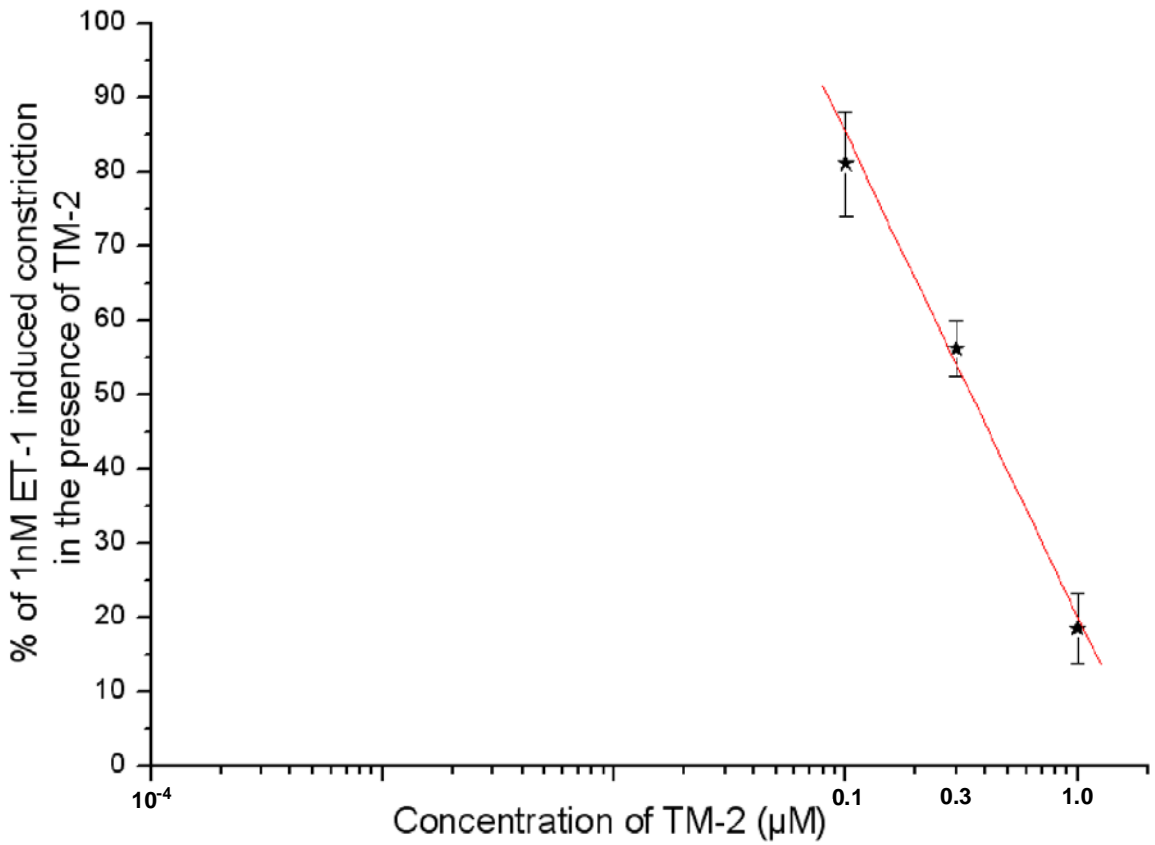
Graph 4. Percentage of 1 nM ET-1 induced constriction in the presence of TM-1 **Versus** concentration of TM-1 (linear)



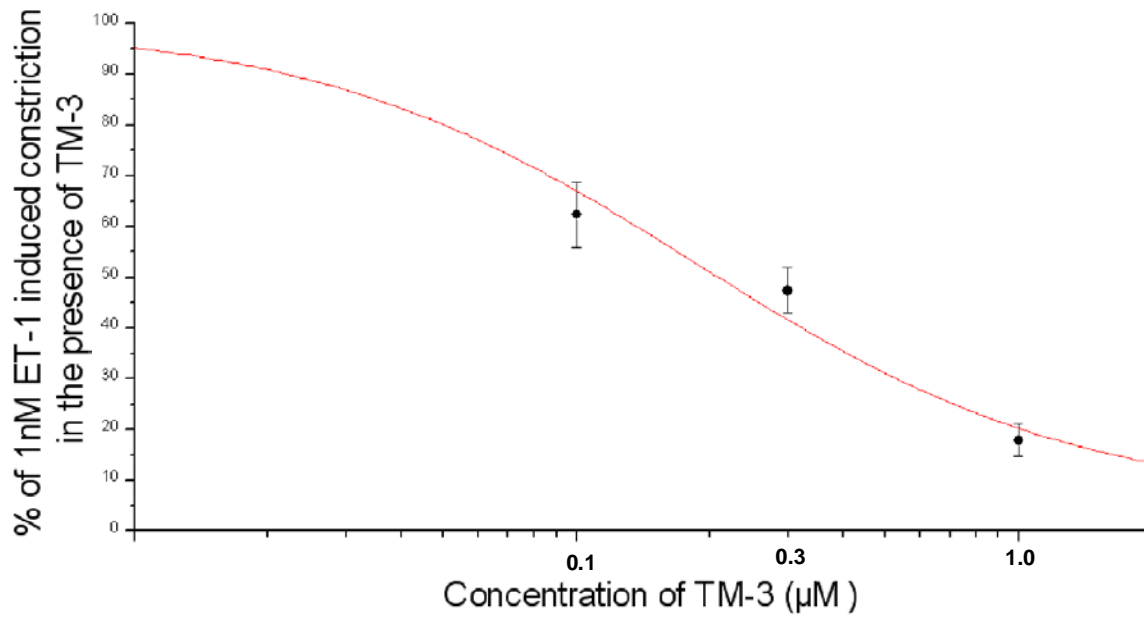
Graph 5. Percentage of 1 nM ET-1 induced constriction in the presence of TM-2 **Versus** concentration of TM-2 (curve)



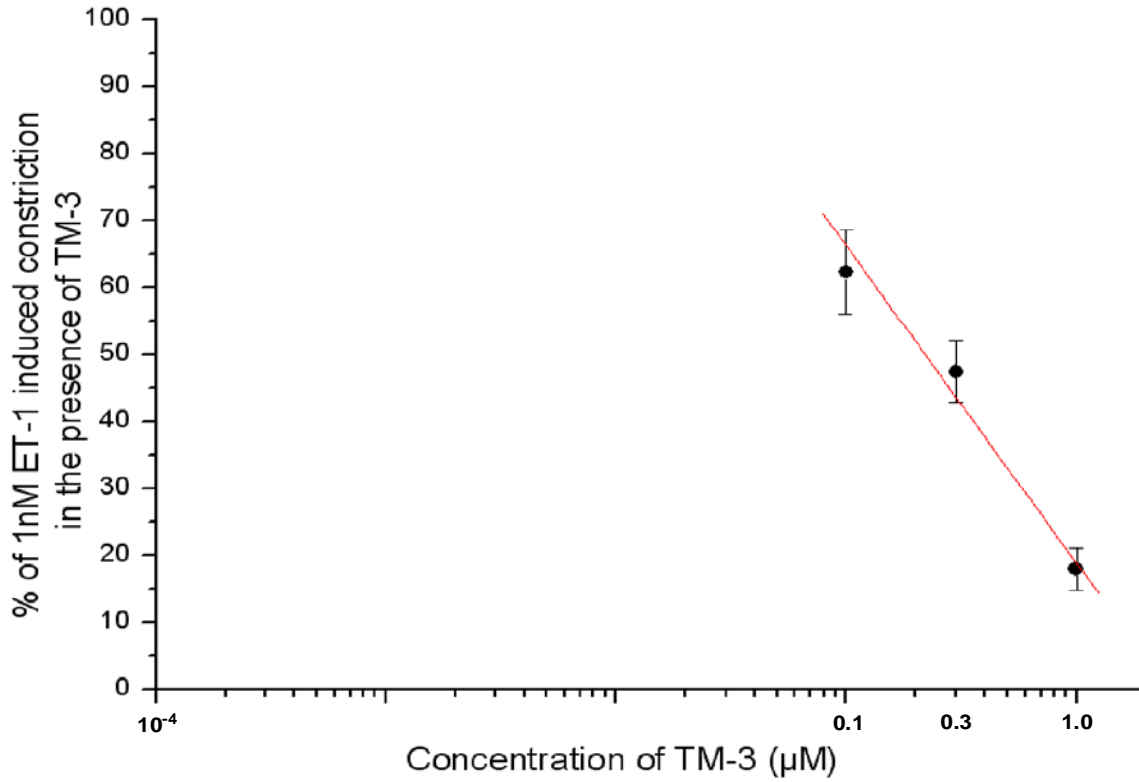
Graph 6. Percentage of 1 nM ET-1 induced constriction in the presence of TM-2 **Versus** concentration of TM-2 (linear)



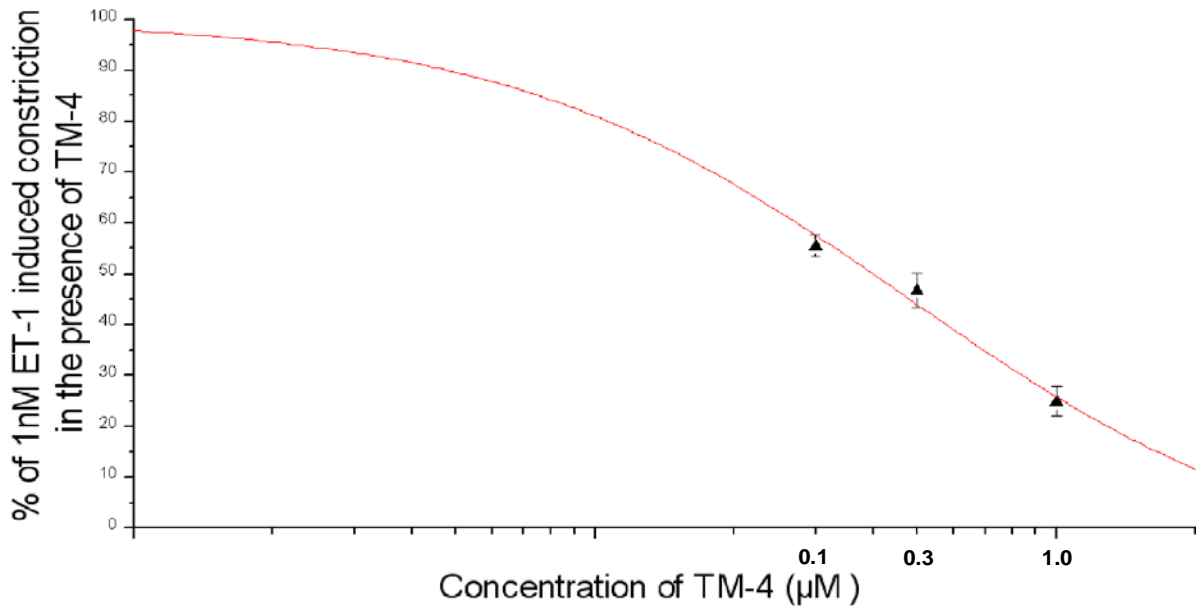
Graph 7. Percentage of 1 nM ET-1 induced constriction in the presence of TM-3 **Versus** concentration of TM-3 (curve)



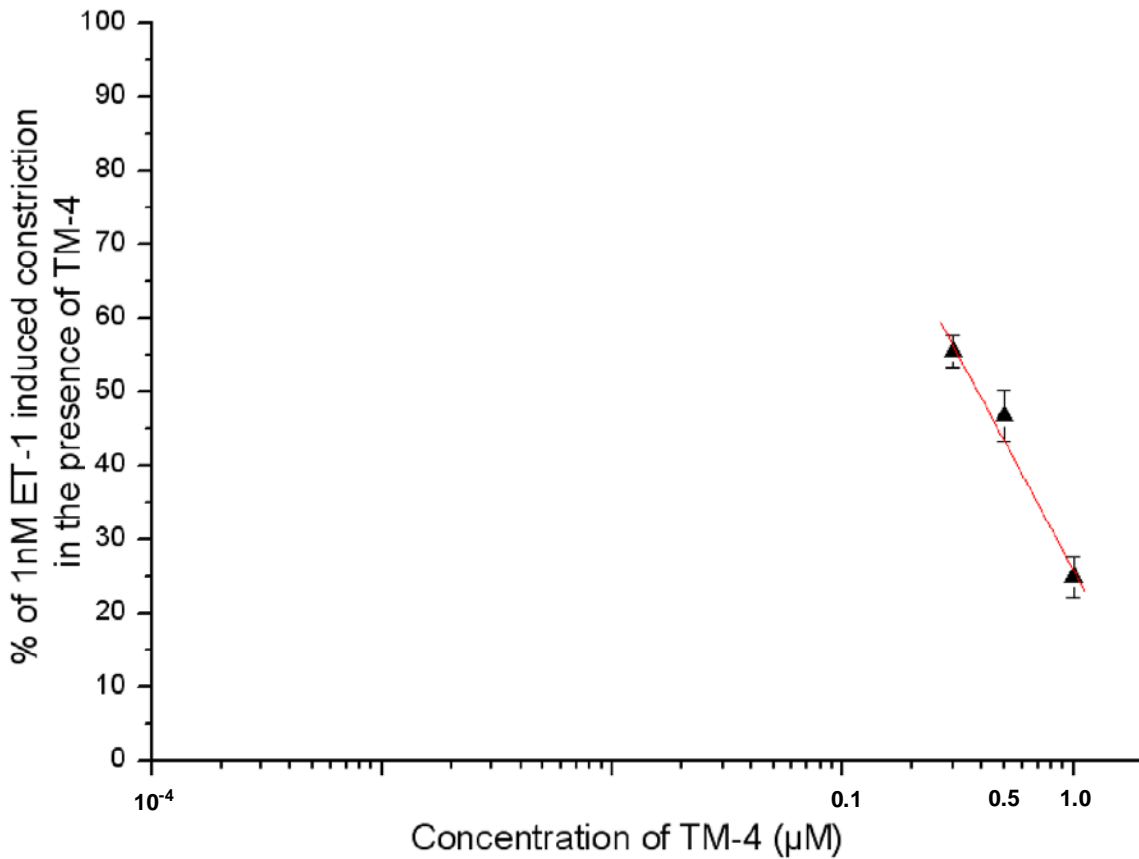
Graph 8. Percentage of 1 nM ET-1 induced constriction in the presence of TM-3 **Versus** concentration of TM-3 (linear)



Graph 9. Percentage of 1 nM ET-1 induced constriction in the presence of TM-4 **Versus** concentration of TM-4 (curve)

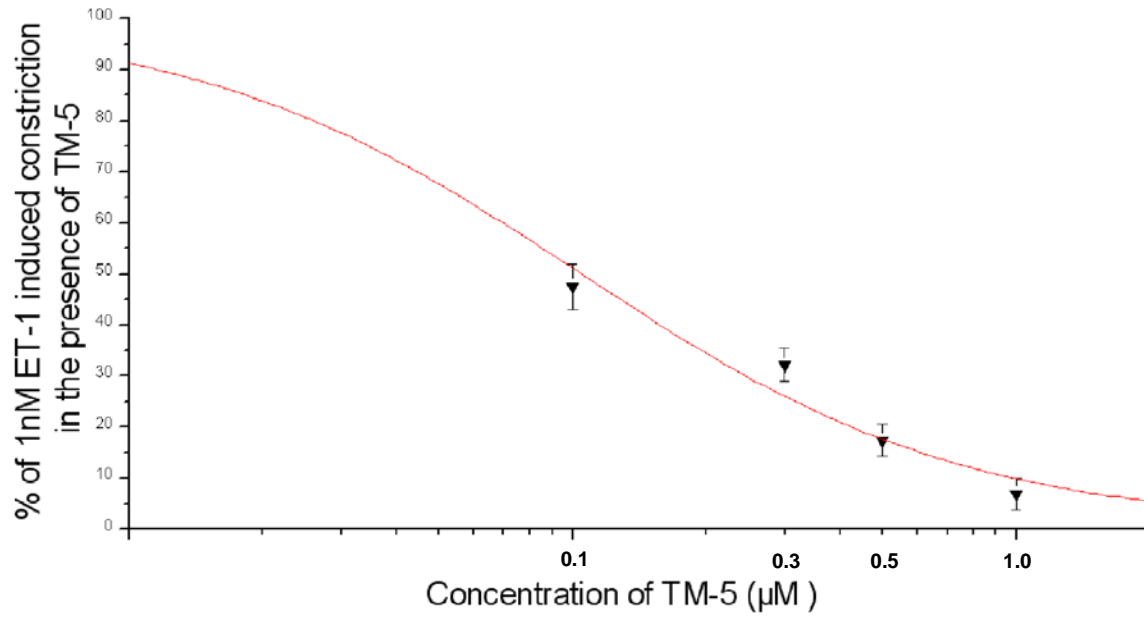


Graph 10. Percentage of 1 nM ET-1 induced constriction in the presence of TM-4 **Versus** concentration of TM-4 (linear)

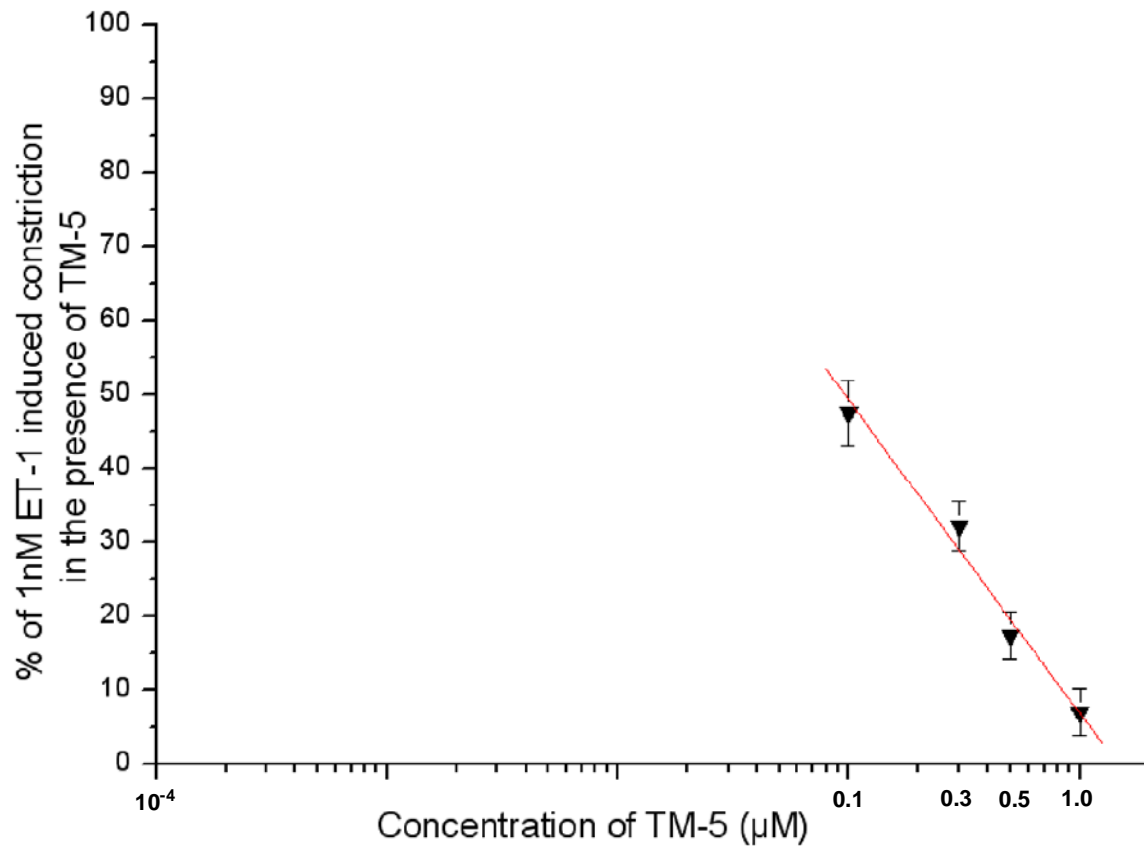




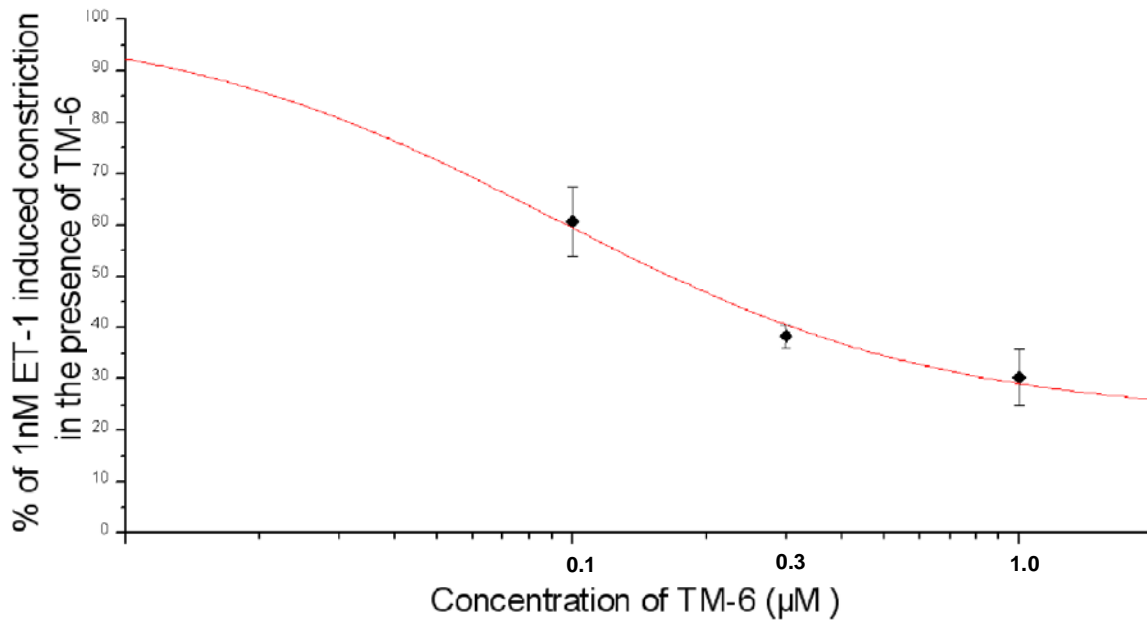
Graph 11. Percentage of 1 nM ET-1 induced constriction in the presence of TM-5 **Versus** concentration of TM-5 (curve)



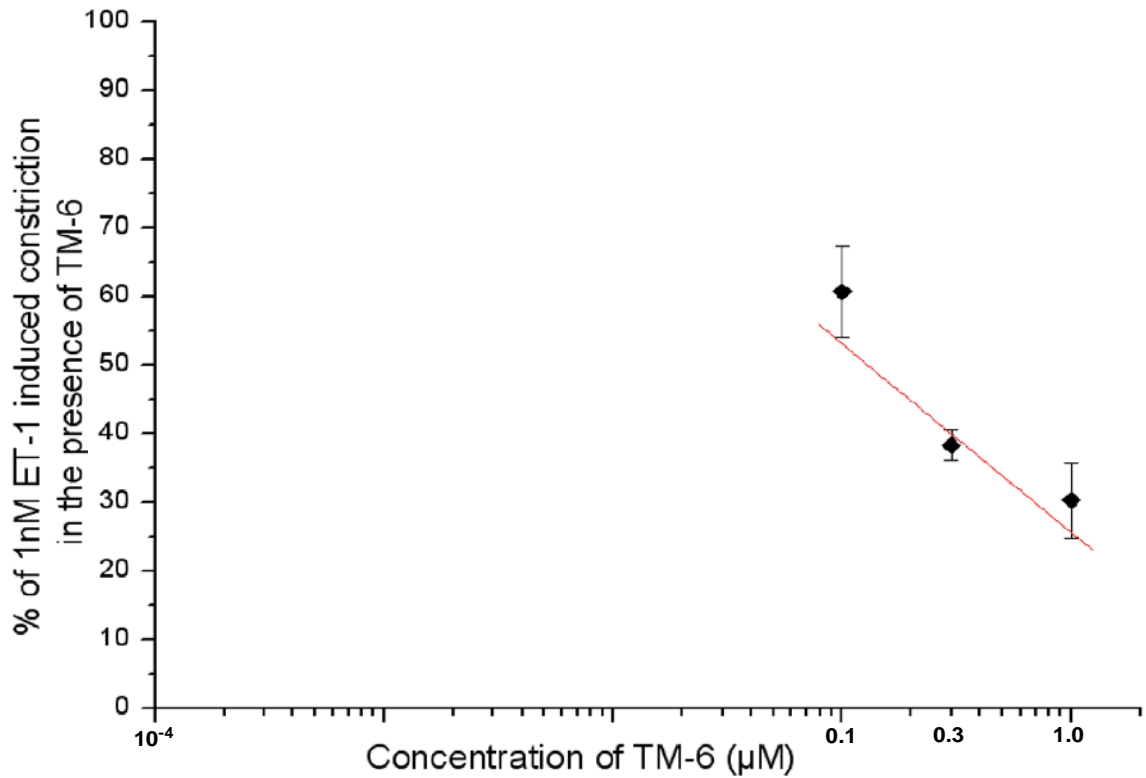
Graph 12. Percentage of 1 nM ET-1 induced constriction in the presence of TM-5 **Versus** concentration of TM-5 (linear)



Graph 13. Percentage of 1 nM ET-1 induced constriction in the presence of TM-6 **Versus** concentration of TM-6 (curve)



Graph 14. Percentage of 1 nM ET-1 induced constriction in the presence of TM-6 **Versus** concentration of TM-6 (linear)



The EC<sub>50</sub> of (+)-myriceric acid A for ET-1 inhibition was reported as 11 nM.<sup>2</sup> The EC<sub>50</sub> of the six (+)-myriceric acid A intermediates calculated by the Origin 6.0 are showed in the below table:

Table 8. Different compound's EC<sub>50</sub> value

<b>Compound Name</b>	<b>half inhibition effect concentration( EC<sub>50</sub>) based on curve relationship</b>	<b>half inhibition effect concentration( EC<sub>50</sub>) based on linear relationship</b>
<b>TM-1</b>	<b>0.185 μM</b>	<b>0.143 μM</b>
<b>TM-2</b>	<b>0.582 μM</b>	<b>0.347 μM</b>
<b>TM-3</b>	<b>0.186 μM</b>	<b>0.220 μM</b>
<b>TM-4</b>	<b>0.475 μM</b>	<b>0.385 μM</b>
<b>TM-5</b>	<b>0.103 μM</b>	<b>0.095 μM</b>
<b>TM-6</b>	<b>0.090 μM</b>	<b>0.129 μM</b>

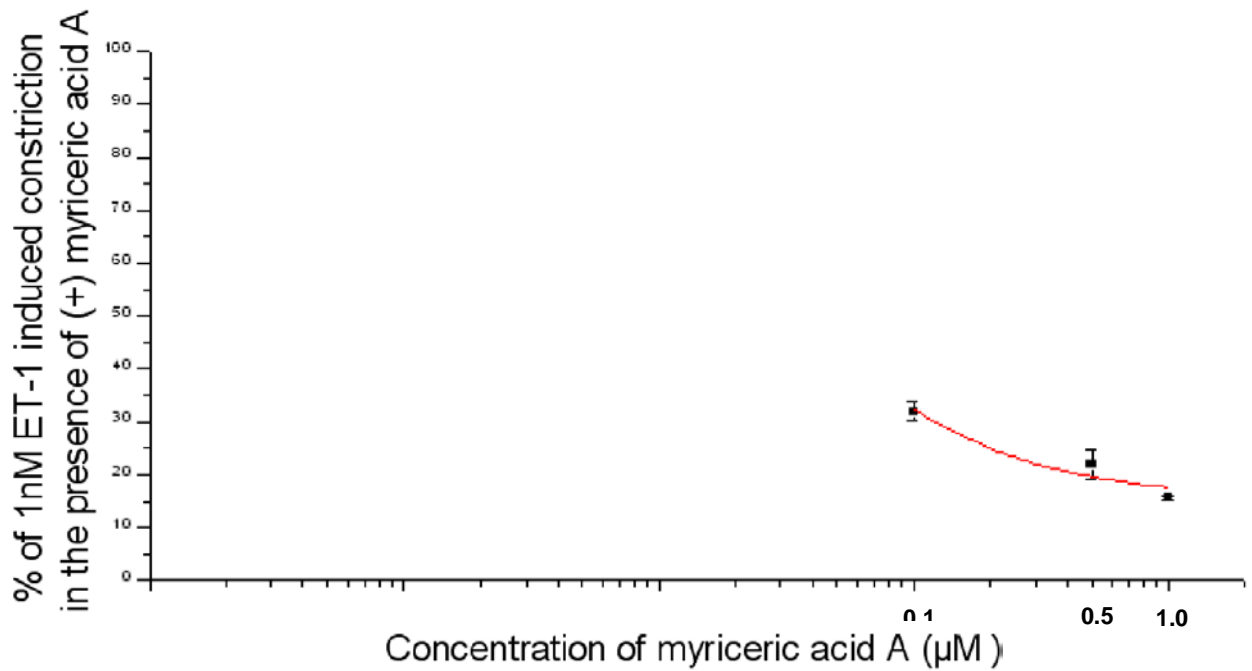
## Chapter 3 Discussion

### 3.1 Comparison of the drug antagonistic potency based on the current result

It is easy to compare the antagonistic potency of (+)-myriceric acid A and its intermediates if their  $EC_{50}$  (half maximal effective concentration) values are calculated.  $EC_{50}$  is the concentration of a compound where 50 percent of its maximal effect is observed. The smaller value of  $EC_{50}$ , the greater antagonistic effect the drug has. The  $EC_{50}$  value of (+)-myriceric acid A is much smaller than its intermediate, so (+)-myriceric acid A has the strongest ET-1 antagonistic potential. ET-1 only exert its vasoconstriction function after it bind with its receptors. The amount of  $ET_B$  receptor is very tiny that discussed in Chapter 1.5.1, so ET-1 binds only with  $ET_A$  receptor. Since (+)-myriceric acid A effectively block the constriction caused by ET-1, hence (+)-myriceric acid A is a potent  $ET_A$  receptor antagonist. According on the result of Table 8 based on curve relationship, the order of the  $EC_{50}$  value for the intermediates is  $TM-6 < TM-5 < TM-1 < TM-3 < TM-4 < TM-2$ . Therefore, the antagonistic potency order for the intermediates should be  $TM-6 > TM-5 > TM-1 > TM-3 > TM-4 > TM-2$ . If the  $EC_{50}$  comparison based on the linear relationship, the order of the  $EC_{50}$  value is  $TM-5 < TM-6 < TM-1 < TM-3 < TM-2 < TM-4$ , so the antagonistic potency order for the intermediates should be  $TM-5 > TM-6 > TM-1 > TM-3 > TM-2 > TM-4$ .

$EC_{50}$  normally is graded in dose-response curves, so it is significant to plot dose-response curves to get  $EC_{50}$  values. However, in order to obtain a good shape dose-response curve in this project, the ET-1 antagonistic effect should be tested under as more as possible concentrations. For example, after scrutinizing Graph 1, it is easy to find that only three concentrations of (+)-myriceric acid A were tested. The dose-response curve was actually elongated in Graph 1. If the curve is cut from the 0.1  $\mu$ M to 1.0  $\mu$ M, the shortened curve is showed in Graph 15 as below:

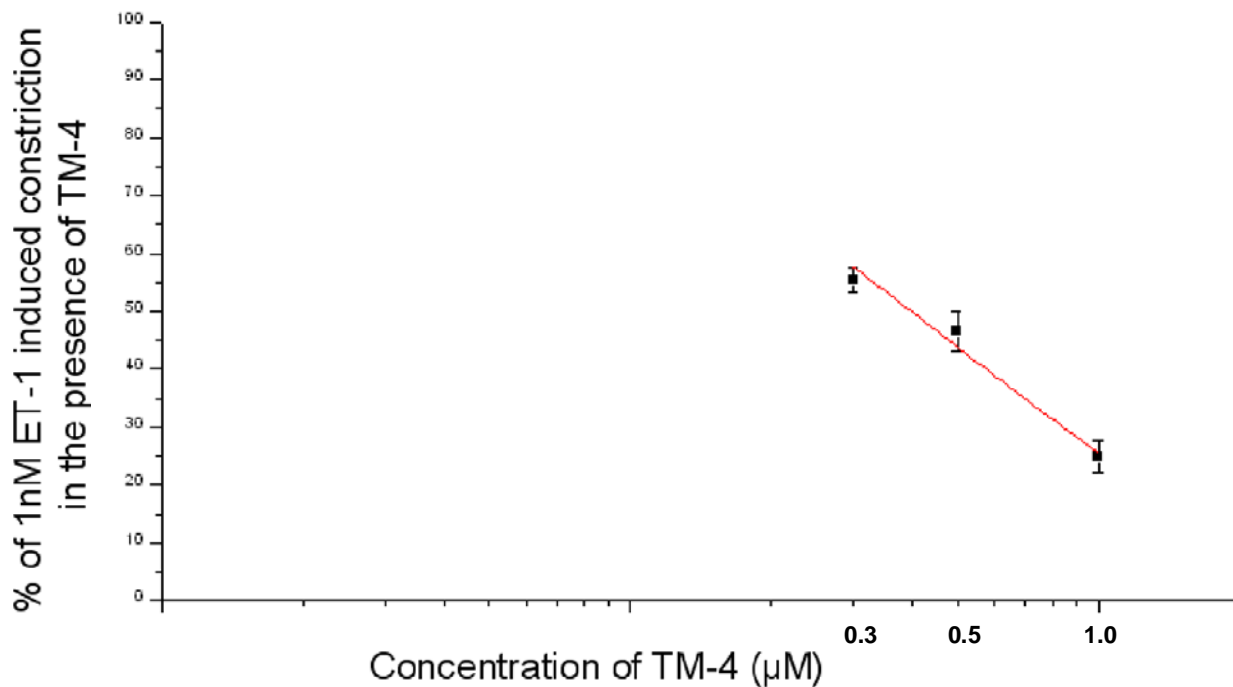
Graph 15. Percentage of 1 nM ET-1 induced constriction in the presence of (+)-myriceric acid A VS Concentration of (+)-myriceric acid A (limited concentration base on curve)



Compared with Graph 1, it is a straight line alike. The scope of the tested concentration was limited between 0.1  $\mu\text{M}$  and 1  $\mu\text{M}$ . It only crossed two decades. The points on the left will definitely change the shape of the curve and influence the  $\text{EC}_{50}$  of (+)-myriceric acid A. So it is wise to test the (+)-myriceric acid A antagonistic effect under at least three decades of concentrations (test less concentrations of (+)-myriceric acid A). If the points at the concentration of 0.01  $\mu\text{M}$  and 0.001  $\mu\text{M}$  (+)-myriceric acid A can be confirmed, a quite good shape and accurate dose-response curve will be plotted. Because of the uncertainty of the curve shape and the current linear shape looking, the linear relationship straight line was plotted

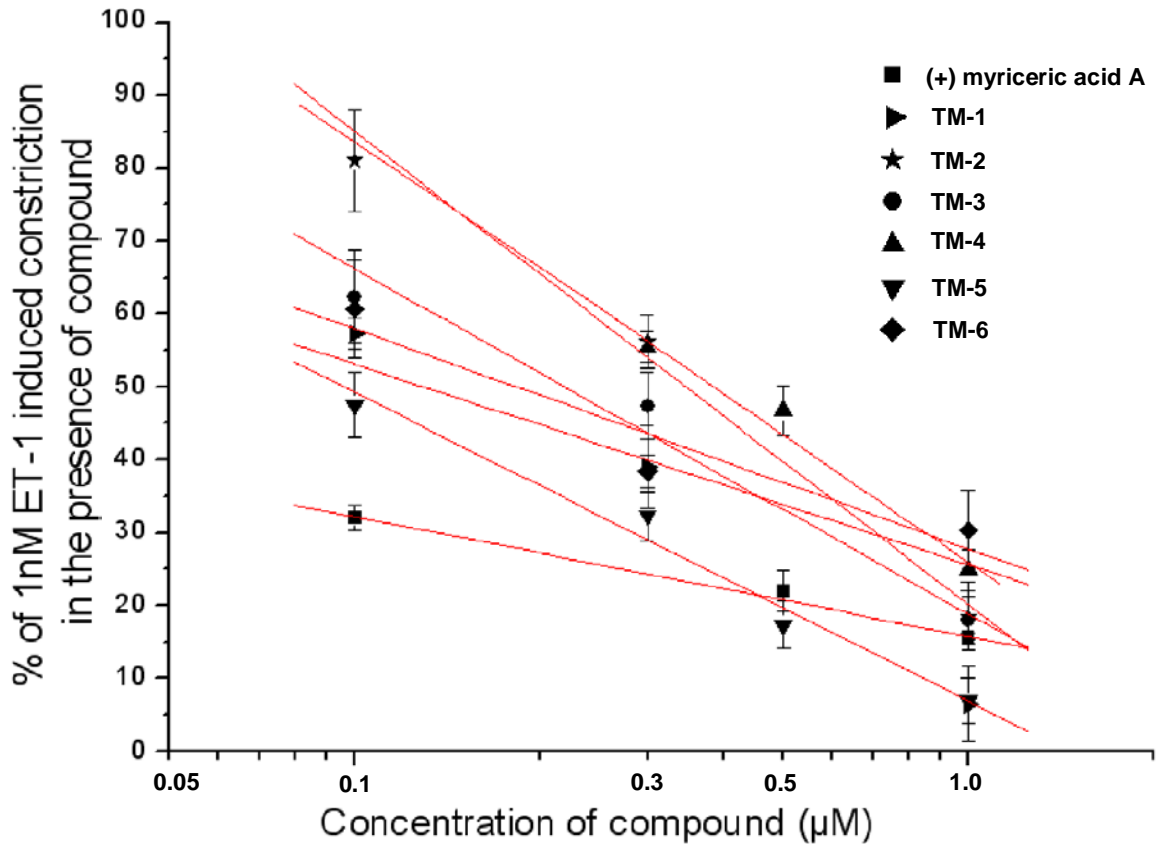
If the curve from 0.3  $\mu\text{M}$  to 1.0  $\mu\text{M}$  of TM-4 is cut, the Graph 16 is showed below:

Graph 16. Percentage of 1 nM ET-1 induced constriction in the presence of TM-4 VS  
Concentration of TM-4 (limited concentration)



The curve in this graph is almost a straight line and the X-Y relationship may be supposed linear. To obtain a complete dose-response curve, more concentrations of compound need to be tested. Based on the current limited data, the linear relationship between concentration of compound and the percent of 1 nM ET-1 induced constriction in the presence of compound is more reasonable. Graph 17 combined all the straight relationship lines together for (+)-myriceric acid A and its six intermediates.

Graph 17. Percentage of 1 nM ET-1 induced constriction in the presence of different compounds VS Concentrations of different compounds (linear)



### 3.2 Some other analysis on the SMA diameter superfusion figures

In this paper, the antagonistic effect of compounds in the presence of 1nM ET-1 is the major concern. It is also important to find out whether these compounds have the ability to reverse the constriction caused by the 1 nM ET-1. In each SMA superfusion experiment, the SMA sections were superfused at least 1 or 2 minutes of 1 mM  $Ca^{2+}$  solution to wash away the ET-1 after the superfusion of ET-1 alone. It is reported that ET-1 can cause a strong and long lasting constriction.<sup>2,3</sup> Including (+)-myriceric acid A and its 6 intermediates, all of them cannot reverse the constriction induced by ET-1 alone.

### 3.3 The simultaneous measurement of intracellular $\text{Ca}^{2+}$ concentration and SMA diameter

In Chapter 1, a proposed mechanism that ET-1 caused vasoconstriction was demonstrated. This mechanism is widely accepted. To normalize the constriction caused by the agonist or the combination of agonist and antagonist, an elevation of the extracellular  $\text{Ca}^{2+}$  concentration from 1 mM to 10 mM  $\text{Ca}^{2+}$  was introduced to induce the increase of intracellular  $\text{Ca}^{2+}$  concentrations.<sup>40</sup> All the procedures are involved the intracellular  $\text{Ca}^{2+}$  concentrations. Scherer et al. developed a simultaneous measurement method to obtain the intracellular  $\text{Ca}^{2+}$  concentrations and SMA diameter. It is quite similar with Figure 8. The only difference is that the SMA segments are loaded with a fluorescent compound (fluo-4) before being mounted in the superfusion chamber and the fluorescence signal can be tested by the connected device to determine the concentration of the intracellular  $\text{Ca}^{2+}$  concentration.

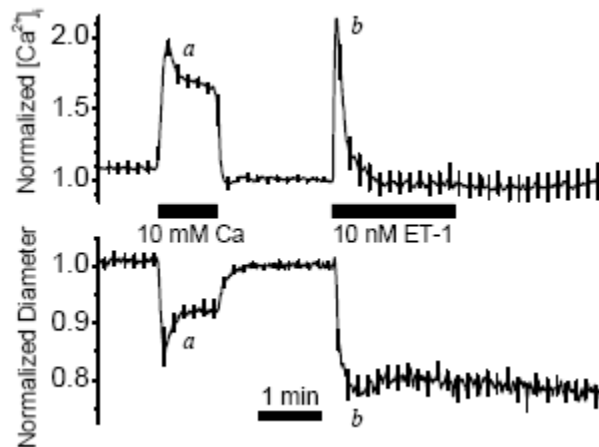


Figure 30. Normalized intracellular  $\text{Ca}^{2+}$  concentration and normalized diameter of SMA in the simultaneous measurement experiment.<sup>34</sup>

The black bars in Figure 30 show the solution superfused at that period.<sup>34</sup> The other periods without black bar means the SMA were superfused 1 mM  $\text{Ca}^{2+}$  solution. At the beginning of the extracellular  $\text{Ca}^{2+}$  concentration elevation from 1 mM to 10 mM, because the  $\text{Ca}^{2+}$  storage in sarcoplasmic reticulum was released due to the stimulation caused by IP3



trigger from the binding ET-1 and ET<sub>A</sub> receptor, the intracellular Ca<sup>2+</sup> concentration had a transient increase. Then it went back a little and kept the same level in the presence of 10 mM Ca<sup>2+</sup> superfusion. When the SMA were superfused with ET-1, the intracellular Ca<sup>2+</sup> concentration sharply increased and quickly went back to the level as it superfused with 1mM Ca<sup>2+</sup> solution. In Chapter 1, it is illustrated that ET-1 will induce the increase of the intracellular Ca<sup>2+</sup> concentration. Therefore, at that time, the SMA constricted. The SMA still constricted and the diameter kept at the same level although the cytosolic Ca<sup>2+</sup> concentration went back very quickly. After superfusion of ET-1, the superfusion of 1 mM Ca<sup>2+</sup> solution can keep the vasoconstriction caused by ET-1 with the unchanged intracellular Ca<sup>2+</sup> concentration. The mechanism of this activity is still unclear.

Scherer *et al.* also devised a cumulative method to test the constriction effect induced by ET-1 on one SMA segment.

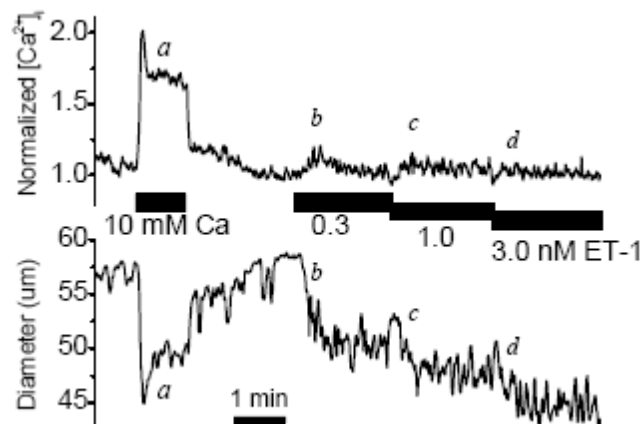


Figure 31. The normalized intracellular Ca<sup>2+</sup> concentration and diameter of SMA in the cumulative simultaneous measurement experiment<sup>34</sup>.

As Figure 31 showed, the intracellular Ca<sup>2+</sup> concentration weren't significantly influenced by the higher concentration of ET-1. However, the diameter of SMA decreased as ET-1's concentration increased.<sup>34</sup>

Looking back at Figure 9, the SMA constricted after being superfused with a combination solution of 1 mM Ca<sup>2+</sup> solution and drug solution. Though the drug had some blocking effect on ET-1, the SMA still constricted. After that period, the diameter of SMA

remained at the same level in the presence of 1 mM  $\text{Ca}^{2+}$  solution superfusion as Figure 30 demonstrated. When SMA was superfused with the same concentration of ET-1, the diameter of SMA decreased a little. This process further proved that the drug had an antagonistic effect. If the drug had no antagonistic effect, the later superfusion of higher concentration of ET-1 wouldn't lead SMA to constrict further, because the ET-1 in the 6<sup>th</sup>~7<sup>th</sup> minute was partially blocked. In other words, during this period, the effective ET-1 concentration was less than the later superfusing ET-1 concentration. The whole process is quite similar as Figure 31 demonstrated.

## **Chapter 4 Conclusion and the prospect of further research**

### **4.1 Conclusion of the current research**

The current experiments demonstrated inspiring information that all six (+)-myriceric acid A intermediates have ET-1 receptor antagonistic effect more or less. Although (+)-myriceric acid A has been proved as ET<sub>A</sub> receptor antagonist, the antagonistic mechanisms of its intermediates are still unclear. In order to compare the antagonistic effect of (+)-myriceric acid A and its intermediates, a dose-response curve was plotted to obtain the EC<sub>50</sub> of each compound. However, because the tested samples were limited and the range of each compound's concentration is narrow, the curve obtained was not perfect, so the linear relationship was proposed. Furthermore, the experimental work further proved that the vasoconstriction caused by ET-1 can be maintained under superfusion of 1 mM Ca<sup>2+</sup> solution.

### **4.2 improvement of future work**

Because only limited numbers of SMA segments were tested at each concentration of drugs, the sample number needs to be increased to improve the result. Furthermore, it is favorable to test more concentrations of compound (at least across 3 decades) to plot better and more reliable dose-response curves.

Although the ET-1 antagonistic mechanisms of these 6 intermediates are not clear, synthesizing these intermediates is easier than the total synthesis of (+)-myriceric acid A. the functional group of each intermediate can be modified to verify which part of the compound is leading to the antagonistic function.

## Reference

1. Fujimoto M., Mihara S., Nakajima S., Nakajima S., Ueda M., Sakurai K., A novel non-peptide endothelin antagonist isolated from bayberry, *Myrica cerifera*. *FEBS Lett.*, **1992**, *305*, 41-44
2. Sakurawi K., Yasuda T., Tozyo T., Nakamura M., Sato T., Kikuchi J., Terui Y., Ikenishi Y., Iwata T., Takahashi K., Konoike T., Mihara S., Fujimoto M., Endothelin receptor antagonist triterpenoid, myriceric acid A, isolated from *Myrica cerifera*, and structure activity relationships of its derivatives. *Chem. Pharm. Bull.*, **1996**, *44*, 343-351.
3. Aguilar Angelo's doctoral dissertation: Progress toward the total synthesis of (+)-myriceric acid A, **2008**
4. Inoue, A., Yanagisawa, M., Kimura, S., Kasuya, Y., Miyauchi, T., Goto, K., Masaki, T., The human endothelin family: three structurally and pharmacologically distinct isopeptides predicted by three separate genes *Proc. Natl. Acad. Sci.*, **1989**, *86*, 2863–2867
5. Nakamuta, M., Takayanagi, R., Sakai, Y., Sakamoto, S., Hagiwara, H., Mizuno, T., Saito, Y., Hirose, S., Yamamoto, M., Nawata, H., Cloning and sequence analysis of a cDNA encoding human non-selective type of endothelin receptor. *Biochem. Biophys. Res. Commun.* **1991**, *177*, 34–39
6. Adachi, M., Yang, Y.Y., Furuichi, Y., Miyamoto, C., Cloning and characterization of cDNA encoding human A-type endothelin receptor., *Biochem. Biophys. Res. Commun.* **1991**, *180*, 1265–1272
7. Cyr, C., Huebner, K., Druck, T., Kris, R., Cloning and chromosomal localization of a human endothelin ET<sub>A</sub> receptor. *Biochem. Biophys. Res. Commun.* **1991**, *181*, 184–190

8. Yanagisawa M., Kurihara H., Kimura S., Tomobe Y., Kobayashi M., Mitsui Y., Yazaki Y., Goto K., Masaki T., A novel potent vasoconstrictor peptide produced by vascular endothelial cells. *Nature*, **1988**, 332, 411-415.
9. Webb M. L., Meek T. D., Inhibitors of endothelin. *Med. Res. Rev.*, **1997**, 17, 17-67.
10. T. Sakurai, M. Yanagisawa, A. Inoue, U. S. Ryan, S. Kimura, Y. Mitsui, K. Goto, and T. Masaki., cDNA cloning, sequence analysis and tissue distribution of rat preproendothelin-1 mRNA. *Biochem. Biophys. Res. Commun.*, **1991**, 175, 44.
11. J. R. Vane, E. A. Anggard, and R. M. Botting., Regulatory functions of the vascular endothelium. *Engl. J. Med.*, **1990**, 323, 27.
12. D. J. Webb, Endothelin receptors cloned, endothelin converting enzyme characterized and pathophysiological roles for endothelin proposed. *Trends Pharmacol. Sci.*, **1991**, 12, 43.
13. M. Yanagisawa, A. Inoue, T. Ishikawa, Y. Kasuya, S. Kimura, S. Kumagaye, K. Nakajima, T. X. Watanabe, S. Sakakibara, K. Goto, and T. Masaki., Primary structure, synthesis, and biological activity of rat endothelin, an endothelium-derived vasoconstrictor peptide. *Proc. Natl. Acad. Sci.*, **1988**, 85, 6964
14. K. Nakajima, S. Kubo, S.-I. Kumagaye, H. Nishio, M. Tsunemi, T. Inui, H. Kuroda, N. Chino, T.X. Watanabe, T. Kimura, and S. Sakakibara. Structure-activity relationship of endothelin: Importance of charged groups. *Biochem. Biophys. Res. Comm.*, **1989**, 163, 424.
15. J. T. Hunt, V. G. Lee, P.D. Stein, A. Hedberg, E. Liu, C.-K. McMullen, and S. Moreland. Structure-activity relationships of monocyclic endothelin analogs. *Bio-Organic Med. Chem. Lett.*, **1991**, 1, 33
16. J. T. Hunt, SAR of endothelin deduced from monocyclic analogs. *Drug News Perspect.*, **1992**, 5, 78

17. D. J. Webb. Endothelin: from molecule to Man. *Br J Pharmacol.*, **1997**, *44*(1):9-20
18. LaDouceur, D.M., Flynn, M.A., Keiser, J.A., Reynolds, E., Haleen, S.J., ET<sub>A</sub> and ET<sub>B</sub> receptors coexist on rabbit pulmonary artery vascular smooth muscle mediating contraction. *Biochem. Biophys. Res. Commun.*, **1993**, *196*, 209–215
19. Haynes, W.G., Strachan, F.E., Webb, D.J. Endothelin ET<sub>A</sub> and ET<sub>B</sub> receptors cause vasoconstriction of human resistance and capacitance vessels in vivo. *Circulation*, **1995**, *92*, 357–363
20. Pang, C.Y., Zhang, J., Xu, H., Lipa, J.E., Forrest, C.R., Neligan, P.C., Role and mechanism of endothelin-B receptors in mediating ET-1-induced vasoconstriction in pig skin. *Am. J. Physiol.*, **1998**, *275*, R1066–R1074
21. R. A. Spokes, M. A. Ghatei, and S. R. Bloom., Studies with endothelin-3 and endothelin-1 on rat blood pressure and isolated tissues: evidence for multiple endothelin receptor subtypes. *J. Cardiovasc. Pharmacol.*, **1989**, *13*, S191.
22. Hirata Y., Emori T., Eguchi S., Endothelin receptor subtype B mediates synthesis of nitric oxide by cultured bovine endothelin cells. *J. Clin Invest*, **1993**, *91*, 1367-1373
23. R. Clinton Webb, Smooth muscle contraction and relaxation., *Adv. Physiol. Educ.*, **2003**, *27*, 201–206
24. J. Dudel., Calcium dependence of quantal release triggered by graded depolarization pulses to nerve terminals on crayfish and frog muscle. *Pflügers archive European Journal of Physiology*, **1989**, *415*, 289-298
25. [http://www.cvphysiology.com/Blood%20Flow/BF012.htm#Intracellular\\_Mechanisms](http://www.cvphysiology.com/Blood%20Flow/BF012.htm#Intracellular_Mechanisms)

26. <http://www.cvphysiology.com/Blood%20Pressure/BP011b.htm>
27. Goto K, Kasuya Y, Matsuki N, Takuwa Y, Kurihara H, Ishikawa T., Endothelin activates the dihydropyridine-sensitive, voltage-dependent Ca channel in vascular smooth muscle. *Proc. Natl. Acad. Sci.* **1989**, 86, 3915-3918
28. Kasuya Y, Ishikawa T, Yanagisawa M, Kimura S, Goto K, Masaki T. Mechanism of contraction to endothelin in the isolated porcine coronary artery. *Am. J. Physiol*, **1989**, 257, H1828-35
29. <http://www.cvphysiology.com/Blood%20Pressure/BP026.htm>
30. <http://www-neuromus.ucsd.edu/musintro/bridge.shtml>
31. Yoshihiko Chiba, Hiroyasu Sakai, Miwa Misawa. Endothelin-1-induced translocation of RhoA was mediated by endothelin ET<sub>A</sub> receptors in rat bronchial smooth muscle. *European J. Pharmacol*, **2005**, 3, 182-185
32. A. P. Davenport and J. J. Maguire., Is endothelin-induced vasoconstriction mediated only by ET<sub>A</sub> receptors in humans. *Trends Pharmacol.*, **1994**, 15, 9
33. T. Fukami, T. Hayama, K. Niiyama, T. Nagase, T. Mase, K. Fujita, U. Kumagai, Y. Urakawa, M. Ihara, S. Kimura, and M. Yano, Twelfth American Peptide Symposium, Cambridge, MA, June 16, 1991, p. 506
34. Scherer E. Q., Wonneberger K., Wangemann P., Differential desensitization of Ca<sup>2+</sup> mobilization and vasoconstriction by ET<sub>A</sub> receptors in the gerbil spiral modiolar artery. *J. Membrane Biol.*, **2001**, 182, 183-191.
35. Scherer, Elias Q., Herzog ,Michael., Wangemann, Phillne. Endothelin-1-induced vasospasms of spiral modiolar artery are mediated by rho-kinase-induced Ca<sup>2+</sup> sensitization of

contractile apparatus and reversed by calcitonin gene-related Peptide. *Stroke*. **2002**, 33, 2965-2971

36. Quirk, W.S., Laurikainen, E.A., Avinash, G., Nuttall, A.L., and Miller, J.M., The role of endothelin on the regulation of cochlear blood flow. *Assoc. Res. Otolaryngol.* **1992**, 15, 37

37. Jinnouchi, K., Tomiyama, S., Pawankar, R., Ikezono, Y., Yagi, T., Distribution of Endothelin-1-like Activity in the Cochlea of Normal Guinea Pigs. *Acta Otolaryngol.* **1997**, 117, 41-45

38. Sadanaga, M., Liu, J., Wangemann, P. Endothelin-A receptors mediate vasoconstriction of capillaries in the spiral ligament. *Hear. Res.* **1997**, 112, 106-114

39. Ghandour S, Cetinel S, Kurtel H., Endothelin-3 induced mesenteric vasoconstriction and PMN infiltration in the rat small intestine: role of endothelin receptors. *Regul Pept.* **2004**, 119, 125-131

40. Wangemann,P., Cohn, E.S., Gruber, D.D. and Gratton, M.A. Calcium-dependence and nifedipine-sensitivity of tone and contractility in the isolated in vitro superfused spiral modiolar artery. *Assoc. Res. Otolaryngol.* **1998**, 21, 119

41. Wangemann, P., Cohn, E.S., Gruber, D.D. and Gratton, M.A. Ca<sup>2+</sup>-dependence and nifedipine-sensitivity of vascular tone and contractility in the isolated superfused spiral modiolar artery in vitro. *Hear.Res.* **1998**, 118, 90-100

42. Wangemann P., Gruber D. D., The isolated in vitro perfused spiral modiolar artery: pressure dependence of vasoconstriction. *Hear. Res.*,**1998**, 115,113-118.